Transcriptional regulation of *ZIP* genes is independent of local zinc status in Brachypodium shoots upon zinc deficiency and resupply

Sahand Amini[1], Borjana Arsova[2], Sylvie Gobert[3,4], Monique Carnol[5], Bernard Bosman[5], Patrick Motte[1], Michelle Watt[2]*, Marc Hanikenne[1]

[1] InBioS - PhytoSystems, Functional Genomics and Plant Molecular Imaging, University of Liège, Belgium

[2] Root Dynamics Group, IBG-2 – Plant Sciences, Institut für Bio- und Geowissenschaften (IBG), Forschungszentrum Jülich, Germany

[3] Laboratory of Oceanology, MARE Centre, FOCUS, University of Liège, Allée du 6 Août, 15, Sart Tilman, B6c, 4000 Liège, Belgium

[4] Station de Recherches Sous-Marines et Océanographiques (STARESO), Pointe Revellata, BP 33, 20260 Calvi, France

[5] InBioS - PhytoSystems, Laboratory of Plant and Microbial Ecology, Department of Biology, Ecology, Evolution, University of Liège, Belgium

* Present address: School of BioSciences, University of Melbourne, Parkville, VIC, 3010, Australia

Corresponding author: Marc Hanikenne, marc.hanikenne@uliege.be, +32-4-3663844

Running head: Zinc homeostasis in Brachypodium

Keywords: zinc, deficiency, excess, resupply, signaling, dynamics, zinc flux, Brachypodium

Abstract

The biological processes underlying zinc homeostasis are targets for genetic improvement of crops to counter human malnutrition. Detailed phenotyping, ionomic, RNA-Seq analyses and flux measurements with ^{67}Zn isotope revealed whole plant molecular events underlying zinc homeostasis upon varying zinc supply and during zinc resupply to starved *Brachypodium distachyon* (Brachypodium) plants. Although both zinc deficiency and excess hindered Brachypodium growth, accumulation of biomass and micronutrients into roots and shoots differed depending on zinc supply. The zinc resupply dynamics involved 1893 zinc-responsive genes. Multiple ZIP transporter genes and dozens of other genes were rapidly and transiently down-regulated in early stages of zinc resupply, suggesting a transient zinc shock, sensed locally in roots. Notably genes with identical regulation were observed in shoots without zinc accumulation, pointing to root-to-shoot signals mediating whole plant responses to zinc resupply. Molecular events uncovered in the grass model Brachypodium are useful for the improvement of staple monocots.

Introduction

Plants have developed a sophisticated zinc homeostasis network to ensure appropriate zinc supply to tissues throughout their lifetime in varying environments (Choi & Bird, 2014; Clemens et al., 2002). Zinc is an essential micronutrient with catalytic, regulatory and structural functions in enzymes and proteins (Broadley et al., 2007; Gupta et al., 2016). Zinc availability to plants in soils is limited in large areas worldwide (Alloway, 2008), limiting primary productivity and the nutritional quality of agricultural products. Zinc deficiency in plants leads to multiple defects, including lower activity of zinc-binding enzymes, higher reactive oxygen species (ROS) production due in part to reduced ROS-detoxifying copper/zinc superoxide dismutase activity, iron accumulation, membrane and chlorophyll damage, and decrease in photosynthetic performance (Vallee & Falchuk, 1993). These defects macroscopically show during growth and development (Broadley et al., 2007; Sinclair & Krämer, 2012). Zinc toxicity from excess exposure can also occur in plants, mostly in anthropogenically-perturbed areas (Jensen & Pedersen, 2006). The main zinc toxicity symptoms include reduced growth and yield, iron deficiency and hence chlorosis, as well as interference with magnesium, phosphorus and manganese uptake, and reduced root growth and root hair abnormality (Broadley et al., 2007; Fukao et al., 2011).

Many molecular actors for root zinc uptake and its transport to different organs and organelles have been identified (Ricachenevsky et al., 2015; Sinclair & Krämer, 2012). Among them, the Zinc-regulated transporter (ZRT), Iron-regulated transporter (IRT)-like Protein (ZIP) gene family includes 15 and 12 members in Arabidopsis (*Arabidopsis thaliana*, At) and rice (*Oryza sativa*, Os), 10 and 7 of which are up-regulated in response to zinc deficiency, respectively (Assunção et al., 2010; Huang et al., 2020; Kavitha et al., 2015; Krämer et al., 2007; Ramesh et al., 2003; Ricachenevsky et al., 2015; Yang et al., 2009). Although ZIP transporters are widely studied, their specific physiological roles in plant metal homeostasis are not completely understood. Several ZIPs are hypothesized to be responsible for zinc cellular uptake and influx into the cytosol (Colangelo & Guerinot, 2006). However, they have their own

specialized functionality and localization, and usually display a broad range of metal substrates. Among the monocotyledonous ZIP transporters involved in zinc, as well as other metal, homeostasis are: rice OsIRT1 (Lee & An, 2009), OsZIP1 (Ramesh et al., 2003), OsZIP4 (Ishimaru et al., 2005), OsZIP5 (Lee et al., 2010), and OsZIP8 (Yang et al., 2009), barley HvZIP7 (Tiong et al., 2014), and maize ZmZIP7 (Li et al., 2016). A number of Heavy Metal ATPases (HMAs) are generally responsible for zinc efflux into the apoplast. The Arabidopsis AtHMA2 and AtHMA4 have an important role in zinc root-to-shoot transport (Hussain et al., 2004). OsHMA2 is apparently the only pump serving this function in rice (Baxter et al., 2003; Takahashi et al., 2012). Metal Tolerance Protein (MTP), Major Facilitator Superfamily (MFS)/Zinc-Induced Facilitator (ZIF), Natural Resistance-Associated Macrophage Protein (NRAMP), Plant Cadmium Resistance (PCR), ATP-Binding Cassette (ABC), Yellow Stripe-Like (YSL), and Vacuolar Iron Transport (VIT), are other transporter families, whose some members are involved in zinc and other metal homeostasis in various dicot and monocot species (Hall & Williams, 2003; Ricachenevsky et al., 2015; Sinclair & Krämer, 2012). Moreover, nicotianamine (NA) is an iron, zinc, copper and manganese chelator involved in intracellular, intercellular and long-distance mobility of these metals in monocots and dicots. NA is synthetized by NA Synthase (NAS) and in graminaceous monocot plants (*i.e.* grasses) exclusively, is the precursor for mugineic acid phytosiderophore (PS) synthesis, which are key for iron acquisition but can also bind zinc (Shojima et al., 1990; Takahashi et al., 1999). The contribution of the 4 *NAS* genes in Arabidopsis was characterized in details (Klatte et al., 2009), and the rice *OsNAS3* gene was demonstrated to be respectively up-regulated and down-regulated by zinc deficiency and excess (Ishimaru et al., 2008; Suzuki et al., 2008), indicating similar functionality.

Sensing and signaling of the zinc status within the plant and in its environment, as well as its integration into a transcriptional regulation of downstream players of the zinc homeostasis network are poorly understood in plants. The Arabidopsis AtbZIP19 and AtbZIP23 are the main known regulators of zinc homeostasis in plants. Both belong to the basic leucine zipper domain-containing (bZIP) TF family and regulate the transcription of *ZIP* and *NAS* genes in response to zinc deficiency in Arabidopsis (Assunção et al., 2010). Close homologs from Barley (HvbZIP56, HvbZIP62, Nazri et al., 2017), wheat (*TabZIPF1*

and *TabZIPF4*, Evens et al., 2017) and rice (OsbZIP48 and OsbZIP50, Lilay et al., 2020) could rescue an Arabidopsis *bzip19bzip23* double mutant under zinc deficiency, suggesting a shred function in zinc homeostasis. It is suggested that the Cys/His-rich motif of the AtbZIP19 and AtbZIP23 proteins is involved in zinc sensing via direct zinc binding, which would inactivate these TFs under cellular zinc sufficiency (Assunção et al., 2013; Lilay et al., 2019). In order to discover proteins involved in zinc sensing and signaling in plants, the proteome dynamics upon zinc resupply in zinc-deficient Arabidopsis plants was recently investigated (Arsova et al., 2019). Profiling transcriptome and miRNAome dynamics upon zinc deficiency and zinc re-supply for a few days was also shown to have good potentials to reveal novel zinc-responsive genes and miRNAs in rice (Bandyopadhyay et al., 2017; Zeng et al., 2019).

A large amount of zinc homeostasis research has been carried out on Arabidopsis, and then translated to monocotyledonous crop plants. However, Arabidopsis is not the most suitable model to understand zinc in monocots, principally because grasses and dicots (i) possess divergent developmental and eventually anatomical features, and (ii) employ distinct iron uptake strategies, based on either chelated iron(III) or reduced iron(II) uptake, respectively, resulting in distinct interactions with zinc (Hanikenne et al., in press; Kobayashi & Nishizawa, 2012; Marschner et al., 1986). The latter is indeed very important as evidence indicate the interdependence of zinc and iron homeostasis in Arabidopsis (Arsova et al., 2019; Fukao et al., 2011; Pineau et al., 2012; Scheepers et al., 2020; Shanmugam et al., 2012) and in grasses (Chaney, 1993; Suzuki et al., 2006; Von Wirén et al., 1996). Rice, alternatively, is often used as a model for grasses, but it possesses the unique feature of combining both iron uptake strategies (Ishimaru et al., 2006). Zinc and iron homeostasis in rice is thus not representative of the bulk of other grasses; although zinc and iron cross-homeostasis was also reported in rice (Ishimaru et al., 2008; Kobayashi & Nishizawa, 2012; Ricachenevsky et al., 2011; Saenchai et al., 2016).

In this study, we asked whether novel information on zinc homeostasis in monocots can be obtained by using the grass model *Brachypodium distachyon* (Brachypodium). Being most closely related to wheat and barley among the staple crops, with more similar phenology and root development and

anatomy than rice and maize (Watt et al., 2009), the information obtained has potential for easier transfer to valuable crops. Brachypodium combines many attributes of a good model: small and sequenced genome, short life-cycle (3-6 weeks), easily transformable and genetically tractable (Brkljacic et al., 2011; Vogel et al., 2010). Brachypodium was previously proposed as a model for iron and copper homeostasis studies in grasses (Jung et al., 2014; Yordem et al., 2011).

We examined the response of Brachypodium to zinc excess and deficiency, including detailed growth phenotyping. We present commonalities and divergences in zinc homeostasis and its interactions with other metals, iron in particular, between Brachypodium, Arabidopsis and rice. Additionally, ionome and transcriptome dynamics of Brachypodium upon zinc resupply of zinc-deficient plants shed light on striking aspects of zinc homeostasis in this species: a transient down-regulation followed by up-regulation of *ZIP* and 83 additional genes in roots at early time-points (10-30 minutes) upon zinc resupply, assimilated to a local zinc shock response, and a similar response of *ZIP* and 15 other genes in shoots in the absence of zinc accumulation, an indication of rapid root-to-shoot signaling during zinc resupply.

Materials and Methods

Plant material, growth conditions and zinc isotopic labeling

Brachypodium distachyon Bd21-3 seeds were used (Vogel et al., 2010). De-husked seeds were surface-sterilized by 70% ethanol for 30 seconds, and 50% sodium hypochlorite and 0.1% Triton X-100 for five minutes. After five washing with sterile water, seeds were stratified in sterile water and in the dark for one week at 4°C. Thereafter, seeds were germinated in the dark at room temperature on wet filter paper for three days. Upon germination, seedlings were transplanted in hydroponic trays and control modified Hoagland medium containing 1 µM zinc ($ZnSO_4$) and 10 µM Fe(III)-HBED (Scheepers et al., 2020) for one week. Then 10-day-old Brachypodium seedlings were grown in control or treatment conditions in hydroponic media for three weeks. Three static conditions were used: control condition (1.5 µM zinc), deficiency (0 µM zinc), and excess (20 µM zinc). In addition, after three weeks of zinc

deficiency, zinc-starved plants were resupplied with 1 µM zinc and then harvested 10 minutes (10 min), or 30 min, or 2 hours (2 h) or 8 h post resupply to capture the dynamic response to a change in zinc supply. Fresh media were replaced each week and last replaced the day before harvest. Harvest took place in a 2h window at day end. The growth conditions were 16 h light per day at 150 µmol m^{-2} s^{-1}, 24°C. In all experiments and conditions, hydroponic trays and solution containers were washed prior use with 6N hydrochloric acid to eliminate zinc traces. This procedure was applied in three independent experiments and the replication level of each analysis is detailed in figure legends. In experiment 1, samples were separately collected for (i) root and shoot phenotyping (Fig. 1 to 3 and S1, S10), (ii) ionome profiling (Fig. 4, 5 and S2, S3) and (iii) RNA-Sequencing (Fig. 6-8 and S4-S7, Table 1, Data S1-S5). Root length measurements were performed using the WinRhizo (Regent Instrument Inc., QC Canada) and PaintRhizo (Nagel et al., 2009) tools. Shoot measurements were performed using a LI-3100C Area Meter (LI-COR, NE, USA). Experiment 2 was performed as experiment 1, with the exception that zinc excess was omitted, for independent confirmation of gene expression profiles (Fig. 9). Finally, in experiment 3, static conditions were 0 µM zinc and 1.5 µM zinc as above, and additionally included 1.5 µM of a heavy non-radioactive isotope of zinc (^{67}Zn, Isoflex, CA, USA, catalog Nr. 200121-01). Zinc-starved plants were resupplied and labelled with 1 µM $^{67}ZnSO_4$, and then harvested at six time-points upon resupply: 10 min, 30 min, 1 h, 2 h, 5 h and 8 h. The isotope-enriched ^{67}Zn solution (25 mM) was prepared by dissolving metal ingot in diluted H_2SO_4 (Benedicto et al., 2011). In experiment 3, samples were separately collected for (i) isotope concentration analysis and (ii) gene expression profiling by qPCR (Fig. 10 and S8, S9, Data S6).

Ionome profiling

Upon harvest, plant root and shoot material were dried at 50°C for four days and then digested with nitric acid (Nouet et al., 2015). In experiment 1, ionome profiling was performed by inductively coupled plasma atomic emission spectroscopy (ICP-OES, Vista AX, Varian, CA, USA; Nouet et al., 2015). In experiment 3, ^{67}Zn, as well as ^{66}Zn, barium and vanadium (as negative controls) concentrations were

measured by Inductively Coupled Plasma Mass Spectrometry using Dynamic Reaction Cell technology (ICP-MS ELAN DRC II, PerkinElmer Inc., MA, USA) (Benedicto et al., 2011).

Quantitative RT-PCR

Upon harvest, tissues were snap frozen in liquid nitrogen and stored at -80°C. Total RNAs were extracted from root and shoot samples, cDNA preparation and quantitative RT-PCR were conducted as described (Spielmann et al., 2020). Relative transcript level normalization was performed with the $2^{-\Delta\Delta Ct}$ method using *UBC18* (Bradi4g00660) and *EF1α* (Bradi1g06860) reference genes for normalization (Hong et al., 2008). Primers pairs and their efficiency are provided in Table S1.

RNA sequencing

42 RNA samples from experiment 1 were used for mRNA-Seq library preparation using the TruSeq Stranded mRNA Library Prep Kit (Illumina, CA, USA). Libraries were multiplexed and single-end 100 nt RNA-Seq was performed on a Novaseq 6000 at the GIGA Center (University of Liege, Belgium) yielding on average ~18 million reads per sample. Raw read sequences were archived at NCBI (Bioproject PRJNA669627). The FastQC software v.0.10.1 (http://www.bioinformatics.babraham.ac.uk/projects/fastqc/) was used for assessing read quality. Trimmomatic tool v.0.32 (Bolger et al., 2014)) was used for removing sequencing adaptors, polyA and low-quality sequences with the following parameters: remove any reads with base with Q < 25 in any sliding window of 10 bases, set crop parameter to 98, leading and trailing to 25, and minimum length to 90 bases. These parameters discarded ~2% of all reads. Using the HISAT2 software v.20.6 (Pertea et al., 2016), reads were mapped on the Brachypodium genome (v.3.2 downloaded from the Phytozome v13 database on 14/02/2020) with --max-intronlen 30000. The average “overall alignment rate” was 93.87% and 98.51% for root and shoot reads, respectively. Finally, mapped read counts (Data S1) were calculated using HTSEQ-COUNT v.0.6.1p1 (Anders et al., 2014).

Data analysis

The DESEQ2 package v.1.26.0 in R v.3.6.2 (Love et al., 2014) was used for normalizing count data, identification of differentially expressed genes (DEG) with a threshold of absolute fold change of +/- 2 and adjusted (Benjamini-Hochberg multiple testing corrected) *p*-value < 0.05, and for principal component analysis (PCA). Gene ontology (GO) enrichment study was performed using the g:GOSt tool embedded in the g:Profiler web server (Raudvere et al., 2019) with threshold of adjusted *p*-value < 0.05, and then visualized with R. For DEG *k*-means clustering, the multiple experiment viewer (MeV) tool was used (Howe et al., 2011). Other statistical tests were conducted using ANOVA or Student's T-test (see Figure legends).

Results

Zinc deficiency and excess hindered Brachypodium shoot growth

Zinc deficiency and excess treatments had negative effects on shoots. Zinc-deficient plants were slightly chlorotic and were shorter than control plants (Fig. 1A), with 22.7% and 27.6% reduction of shoot fresh and dry weight (Fig. 2A-B), as well as 17.5% smaller total leaf area (Fig. 2C). Interestingly, zinc-deficient plants had as median two leaves more than control plants (Fig2D), but with 26.8% lower dry weight per leaf (Fig. S1A).

Similarly, excess zinc impeded shoot growth and caused leaf chlorosis, but with more severe effects than deficiency (Fig. 1A). Shoot fresh and dry weight as well as total leaf area were 47.7 to 56.2% lower in excess condition compared to control and deficiency (Fig. 2A-C). Plants grown in excess had as median three and five leaves less than control and deficiency plants, respectively (Fig. 2D). Finally, dry weight per leaf of zinc excess plants was 34.3% lower than control plants but the difference with zinc-deficient plants was non-significant (Fig. S1A).

Zinc deficiency and excess altered root phenotypes of Brachypodium plants

209 The zinc effect on root growth of Brachypodium plants (Fig. 1B) differed to shoot responses. Under
210 deficiency, root fresh and dry weight, as well as total root length were reduced by 15.2 to 16.5% (Fig.
211 3A-C). Lateral root length was driving the difference in total root length (Fig. 3D), as it was reduced by
212 17% while primary root lengths were similar under deficiency and control. Zinc-deficient plants had
213 developed one less nodal root (Fig. 3E) and lower total nodal root length (Fig. S1B) than control plants.

214 Zinc excess plants had 22.3 to 38% lower fresh and dry root weight than control and zinc-deficient
215 plants (Fig. 3A-B), exhibiting stronger responses than the deficiency treatment for these traits. Plants
216 had reduced total root length (Fig. 3C), and slightly (but non-significantly) longer primary roots (Fig.
217 3D). Total length of lateral roots of zinc excess plants was 5.2% lower than control, but 14.2% higher
218 than in zinc-deficient plants (Fig. 3D). Finally, zinc excess fully inhibited nodal root growth (Fig. 3E and
219 Fig. S1B).

220 **Zinc deficiency and excess impacted the ionome in Brachypodium**

221 Roots and shoots of zinc-deficient plants had 14.7 and 4.4 times lower zinc concentrations than control
222 plants, respectively (Fig. 4A-B). Zinc excess caused higher zinc accumulation in roots, with 18.6 time
223 greater concentration than in control plants (Fig. 4A). Zinc accumulation in shoots of excess plants was
224 ~4.2 fold higher than in control plants (Fig. 4B). Higher zinc supply corresponded to a greater ratio of
225 root to shoot zinc concentration in Brachypodium, indicating different zinc allocation to the tissues
226 under the different zinc regimes (Fig. 4C).

227 Zinc deficiency and/or excess also affected iron, manganese, copper, calcium and magnesium
228 concentrations in Brachypodium tissues (Fig. S2). Manganese and copper were slightly but significantly
229 less abundant in roots upon deficiency (Fig. S2C,E). Root iron and shoot copper concentrations of zinc-
230 deficient plants were 40.7% increased or 25.3% decreased, respectively (Fig. S2A,F). Notably, upon zinc
231 excess, manganese and copper root concentrations were 3.4 and 2.1-fold reduced compared to
232 control, respectively (Fig. S2C,E). Finally, calcium and magnesium were 33% and 35.1% higher in shoots
233 of zinc excess plants, respectively (Fig. S2H,J).

Rapid ionome dynamics was observed in Brachypodium roots upon zinc deficiency and resupply

During zinc resupply of zinc deficient roots, we observed gradual accumulation of zinc through time. Zinc increase was modest and non-significant after 10 and 30 min, but reached 3.7-fold after 8 h (Fig. 5A). In contrast to the roots, shoot zinc had no consistent increase within the 8 h of re-supply (Fig. 5A).

Zinc resupply affected the whole ionome (Fig. 5 and Fig. S3). The root iron concentration rose gradually until 2 h parallel to increased zinc level (Fig. 5B). Copper and manganese root concentrations displayed different dynamics to zinc and iron with higher levels after 10 min, but a severe and transient drop at the 30 min time-point (Fig. 5C-D). Changes in the shoot ionome were minor (Fig. 5B-D).

Transcriptomic responses to steady-state zinc deficiency and excess and to dynamic zinc deficiency and resupply

Principal component analysis (PCA) of the RNA-Seq data indicated that gene expression variance between biological replicates was very low, with the exception of 30 min resupply shoot samples (Fig. 6A-B and S4). In roots (Fig. 6A), samples clustered according to root zinc concentration (Fig. 4, 5). Control and zinc excess samples were similar and zinc deficiency samples distinct (Fig. 6A). Samples collected after 10 min and 30 min of resupply were similar but distinct from deficiency samples. The 2 h and 8 h resupply samples that contained relatively higher zinc concentrations further clustered separately (Fig. 6A). The shoot PCA component(s) affecting sample clustering are more difficult to interpret (Fig. 6B), possibly in relation to the delayed zinc shoot accumulation (Fig. 5A) and therefore lower impact of zinc concentration as a principal component. However, even in shoot, PCA separation between static and resupply samples is clear along PC1, with static conditions on the x-axis left side while resupply samples are progressing with time towards the right along the x-axis (Fig. 6B).

Differentially expressed genes (DEG) were identified [adjusted $p < 0.05$ and $\log_2$(fold change) > 1] in a selection of 9 out of 21 possible contrasts between the seven treatments for roots and shoots. The 9 contrasts included comparisons of zinc deficiency and excess to the control (2 comparisons), of zinc resupply time-points to deficiency (4 comparisons), and between consecutive resupply time-points (3

comparisons) (Fig. 6C). 1215 and 976 unique DEG were identified in roots and shoots, respectively. 298 genes were common among roots and shoots, meaning that 1893 unique DEG appeared in 9 contrasts (Data S2). The steady-state responses to zinc deficiency and excess mobilized less DEG than the dynamic response to zinc resupply. There was little overlap in the zinc resupply response between roots and shoots (Fig. 6D). The transcriptional response to zinc resupply was rapid and massive in roots, with the up- or down-regulation of > 450 genes within 10 min (Fig. 6C), with only a small overlap (2.4%) with static deficiency response (Fig. 6D). This latter figure was higher for shoots (9.8%) but differential expression between deficiency and 10 minutes of zinc resupply concerned many genes as well. In roots and shoots, the response to zinc resupply continued to mobilize new genes with time, but slowed down, with a remarkable low number of DEG between the 2- and 8 h time-points (Fig. 6-C-D).

Unique biological pathways were involved in the dynamic response to Zn resupply compared to steady-state zinc deficiency and excess

DEG, up-regulated and down-regulated, were submitted to Gene Ontology (GO) enrichment analyses. Over-represented biological processes (BPs, *p*-value < 0.05) were identified in most contrasts (Fig. 7, Data S3).

The “zinc ion transport” BP was strongly overrepresented among DEGs in roots and shoots of deficient plants (0 vs 1.5 µM zinc), with only up-regulated genes, whereas overrepresentation of catabolism, oxidation-reduction and response to chemical processes was observed in response to excess (20 vs 1.5 µM zinc) in roots, driven by down-regulated genes only (Fig. 7A).

The dynamic response to zinc resupply mobilized many more BPs. In roots, multiple enriched BPs corresponding to up-regulated genes were noticeable (high density red color, Fig. 7A) at the 10 min and/or 30 min time-points compared to deficiency. These BPs were mainly related to signaling, different metabolisms, and stress and hormone responses. “Transcription” as well as other signaling-related BPs were enriched only after 10 min resupply. Noticeably, a single enriched BP, “divalent metal transport”, corresponded to down-regulated genes at 10 min (blue cell at “10 min vs 0 µM zinc”). This

item, as well as "zinc ion transport", was also enriched with down-regulated genes (blue cells) after 2 h of zinc resupply compared to deficiency. As expected, the genes corresponding to the "zinc ion transport" BP were strongly up-regulated at deficiency, but were down-regulated within 2 h upon resupply. Finally, a single or no BP were enriched in "30 vs 10 min" and "8 vs 2 h" consecutive time-point comparisons, respectively, whereas a shift in the zinc resupply response was observed between 30 min and 2 h, with many of the early up-regulated genes being down-regulated in that interval (see the blue cells in the "2 h vs 30 min" comparison, Fig. 7A).

In shoots (Fig. 7B, Data S3), the most striking observation was an enrichment of "zinc ion transport", "divalent metal ion transport" and "cation transmembrane transport" BPs, corresponding to down-regulated genes within 10 min of resupply, suggesting that a quick transcriptomic regulation of zinc transporter genes preceded zinc re-entry in shoots (Fig. 5A). This response was transient as the enriched "zinc ion transport" BP corresponded to up-regulated genes (30 min) and then down-regulated genes (2 and 8 h) upon resupply compared to deficiency, respectively. Enriched BPs related to transcription, stress and hormone responses, cellular metabolism and regulation, as well as photosynthesis (Fig. 7A, up-regulated BPs, in red), most of which appeared after 10 min resupply in roots, were observed after 30 min in shoots (Fig. 7B), i.e. with one time-point delay.

Genes encoding members of all zinc transporter families were differentially regulated through time and throughout the different conditions

Among the 1893 identified DEG (Fig. 6), 27 genes were related to zinc/iron/copper/manganese/cadmium homeostasis/resistance, based Phytozome BLAST annotation (Table 1). As Brachypodium is a relatively new model and metal homeostasis studies on this species are scarce, the majority of these annotations were based on sequence or domain similarities with genes/proteins of other species, especially Arabidopsis and rice. Among these 27 genes, 19 genes were differentially expressed in roots only, 2 in shoots only and 6 in both tissues (Table 1). The transcriptional regulation of these genes among the 9 selected contrasts is provided in Fig. S5. The 27 genes belong

309 to families of metal transporters [ZIP (8 genes), MTP (1 gene), HMA (1 gene), NRAMP (1 gene), VIT (1
310 gene), PCR (1 gene), ABC transporter (1 gene)], metal chelator synthesis [NAS (1 gene)] and transport
311 [MFS/ZIF (2 genes), YSL (2 genes)] or metal chaperones [ATX (1 gene), ATOX1/HIPP (7 genes)]. In
312 general, all known and major zinc transporter families (Ricachenevsky et al., 2015; Sinclair & Krämer,
313 2012) had thus at least one representative among DEGs. However, at least some of the 27 DEGs (*e.g.*
314 YSL, NRAMP) may be involved not only in zinc, but also in iron, manganese and/or copper homeostasis.

315 Root and shoot DEG were then clustered according to their expression pattern. Zinc excess was
316 excluded from the analysis as no metal-related genes were regulated in this condition. A total of 9 and
317 8 clusters were obtained for roots and shoots, respectively (Fig. S6, S7, Data S4). Metal homeostasis-
318 related genes were distributed in several clusters, with distinct expression patterns, including early or
319 late responses as well as transient regulation, mostly in roots. For instance, root cluster #3 (127 genes)
320 contained 3 metal homeostasis genes: an *MTP* and 2 copper metallochaperones (Data S4). These genes
321 displayed increased gene expression upon zinc resupply, especially at 2 and 8 h. The six root *ATOX1*-
322 related copper chaperones were distributed in three clusters (#3, #4, #5) which included genes induced
323 with different kinetics during resupply (Fig. S6). In contrast, *YSL* family genes clustered together with
324 genes whose expression was intermediate at deficiency and high in control but was transiently
325 repressed during resupply (Cluster #1, Fig. S6).

326 **Gene clustering showed an unusual temporal regulation of *ZIP* genes upon zinc resupply**

327 Among root clusters (Fig. S6), cluster #2 (91 genes) contained all 8 differentially expressed *ZIP* genes
328 identified in root samples (Table 1), as well as two other metal-related genes (*BdHMA1* and a VIT family
329 gene) (RootZIP cluster, Data S5). Similarly, among shoot clusters (Fig. S7), cluster #4 (21 genes)
330 contained all six *ZIP* genes differentially expressed in shoots (ShootZIP cluster, Data S5). Gene
331 expression patterns in root and shoot ZIP clusters (Fig. 8A-B) had a similar shape with two evident
332 peaks of expression at 0 µM zinc and 30 min and a valley at 10 min, resulting in a V-shape consistent
333 with the observation made in the shoot GO enrichment heatmap for the “zinc ion transport” BP.

Shoot *ZIP* transporter genes are down-regulated before measurable amounts of Zn are transported to the shoot

To confirm the V-shape expression pattern of *ZIP* genes (Fig. 8), a fully independent experiment with the same design was conducted, except with the exclusion of zinc excess (Experiment 2, Methods). Quantitative RT-PCR was used to profile expression of selected genes: (i) *BdZIP4*, *BdZIP7* and *BdZIP13* present in RootZIP and ShootZIP clusters, (ii) *BdIRT1* and *BdHMA1* present in the RootZIP cluster only and (iii) the *NAS* gene that was not present in either of these clusters. Complete consistency was observed between RNA sequencing and qPCR data for all six genes in root and shoot tissues in deficiency, resupply and control (Fig. 9).

The reproducible V-shape expression pattern of *ZIP* family and 15 other genes in the shoot gene cluster #4 long before zinc influx could be detected in shoots (Fig. 5) was puzzling. A possibility was that a tiny amount of zinc was reaching the shoot tissues rapidly, in an amount lower than the ICP-OES detection limit, and was responsible for local transcriptional regulation for these genes. To enable distinction between zinc still present in shoots after 3 weeks of deficiency (~75 ppm, Fig. 5A) and resupplied zinc, ^{67}Zn, a non-radioactive zinc isotope, was used for resupply (Experiment 3, Methods). Note that 1 and 5 h time-points were added to refine the dynamics information. To increase sensitivity and enable detection of zinc isotopes, ^{67}Zn concentration measurements were obtained using ICP-MS.

To ensure that ^{67}Zn has the same physiological effect as naturally abundant zinc, we first analyzed zinc-responsive genes by qPCR (Fig. S8 compared to Fig. 9). The V-shape expression pattern of *BdZIP4*, *BdZIP7* and *BdZIP13* in roots and shoots were again observed. Second, as natural zinc contains a mixture of stable zinc isotopes, with ^{64}Zn being the dominant form and ^{67}Zn representing ~4% (Benedicto et al., 2011), natural zinc supply (1.5 µM) was used as a first negative control (Fig. S9A). In line with our expectations, ^{67}Zn concentrations were low when plants were treated with natural zinc, and even much lower in deficiency (Fig. S9A). Third, ^{66}Zn concentrations in tissues were measured as a second negative control. ^{66}Zn measurements were stable throughout the ^{67}Zn resupply series whereas

359 it was ~7 times higher when plants were treated with natural zinc (Fig. S9B), as described (Benedicto
360 et al., 2011).

361 Next, ^{67}Zn accumulation in isotope-labelled samples was examined (Fig. 10, Data S6). In roots, a gradual
362 and significant increase of ^{67}Zn concentrations was observed with time upon resupply to deficient
363 plants (Fig. 10A, Data S6). The gain in sensitivity compared to Experiment 1 was evident: a significant
364 zinc concentration increase was measured from 10 min (Fig. 10A), when such a change was only
365 detected after 2 h in our initial kinetics (Fig. 5A). In contrast, ^{67}Zn accumulation in shoots was only
366 detected after 5 h (Fig. 10B). Examining shoot to root ^{67}Zn ratios confirmed that starting from a higher
367 ^{67}Zn shoot accumulation in deficiency, ^{67}Zn resupply mostly triggered root accumulation up to 5 h
368 before the ratio stabilized (Fig. 10C).

369 **Discussion**

370 In this study, Brachypodium displayed the typical behavior of a zinc-sensitive, excluder plant (Krämer,
371 2010). It prioritized shoot zinc accumulation upon deficiency and majorly retaining zinc in roots upon
372 excess (Fig. 4), in both cases to preserve the photosynthetic function in leaves. This behavior was very
373 similar to Arabidopsis (Arsova et al., 2019; Talke et al., 2006). However, we showed that the molecular
374 pathways used to achieve this are in part different from Arabidopsis, including distinct interactions
375 (iron) and competition (manganese and copper) with other micronutrients, distinct dynamics of zinc
376 transporter genes and distinct local and systemic signaling.

377 **Zinc deficiency and excess impact growth and development in Brachypodium**

378 In shoots, increased leaf number was peculiarly associated with reduced total leaf area, total leaf
379 biomass and dry weight per leaf in zinc-deficient plants (Fig. 2B-D and Fig. S1A). Leaf number is known
380 to be influenced by multiple factors such as flowering time and nutrition (Durand et al., 2012; Hu et
381 al., 2017; MacFarlane & Burchett, 2002). In our RNA-Seq data, three homologs of rice flowering-
382 promoting genes, *OsFTL12* (Bradi1g38150, shoots) and *OsFPFL1* (Bradi1g18240, shoots) and *OsFTL6*
383 (Bradi3g48036, roots), were highly up-regulated (7-52 fold) upon zinc deficiency (Data S2). This opens

384 the question of the role of zinc in flowering regulation in Brachypodium. Nutrient deficiency is known
385 to accelerate flowering (Kolář & Seňková, 2008), and flowering is linked with shoot size and leaf
386 number in Arabidopsis, although the effect is variable among early and late flowering ecotypes (Chen
387 & Ludewig, 2018). In Brachypodium, clear repression of vegetative growth was associated with
388 increased leaf number. We hypothesize that in order to optimize nutrient use efficiency in shoot and
389 maintain photosynthesis, plants have adjusted leaf area partitioning (Smith et al., 2017).

390 Root types were affected differentially depending on zinc supply. Deficiency and excess treatments
391 increased lateral root number and length relative to the primary root, and nodal roots, post-embryonic
392 shoot-born roots emerging from consecutive shoot nodes and a unique feature of monocots, were
393 strongly affected. Their initiation was fully inhibited upon zinc excess (Fig. 3E). Nodal roots of wheat
394 (Tennant, 1976) are strongly suppressed by low nutrients. In Brachypodium, deprivation of nitrogen,
395 phosphorus (Poiré et al., 2014) and water (Chochois et al., 2015) similarly results in significantly lower
396 number of nodal roots. A positive correlation between nodal root numbers and the nutrient uptake,
397 including nitrogen, phosphorus, iron and zinc, is observed in rice (Subedi et al., 2019). Due to a higher
398 diameter of metaxylem to seminal roots and consequent impact on nutrient uptake capacity, nodal
399 roots play a role in nitrate supply to the plant (Liu et al., 2020; Steffens & Rasmussen, 2016). If this is
400 true for zinc too, the observed absence of nodal roots during zinc toxicity can be interpreted as a
401 protective mechanism that minimizes zinc uptake into the plant. However, the decreased number of
402 nodal roots during deficiency does not fully fit into this narrative, unless the development of nodal
403 roots itself has specific zinc requirements. Furthermore, nodal roots provide mechanical stability to
404 the plant (e.g. from winds, Liu et al., 2020), the decreased number or absence of nodal roots in soils
405 with unfavorable zinc conditions may prove to be disadvantageous to logging in various crops and thus
406 further increase of yield loss (in addition to the physiological zinc effects). It would therefpre be
407 interesting to look for variation in nodal root allocation in response to zinc among Brachypodium
408 accessions, as was found for water supply (Chochois et al., 2015).

Interaction of zinc and other metal homeostasis

Zinc excess had no impact on iron root and shoot levels in Brachypodium (Fig. S2A) and no enrichment for iron homeostasis genes was observed in the transcriptomic response to zinc excess (Fig. 7, Data S2). This contrasts with results from Arabidopsis where zinc excess triggers a secondary iron deficiency with a strong transcriptional response, and zinc toxicity symptoms can be alleviated by higher iron supply (Fukao et al., 2011; Hanikenne et al., in press; Lešková et al., 2017; Shanmugam et al., 2012; Zargar et al., 2015). The iron accumulation dynamics in Brachypodium roots was also in contrast to Arabidopsis with a transient increase upon zinc resupply (Fig. 5B). Zinc deficiency and resupply instead induces a transient decrease in iron concentration in roots of Arabidopsis (Arsova et al., 2019).

Differences to Arabidopsis studies may be because dicot plants and grasses use distinct iron uptake systems (Kobayashi et al., 2012; Hanikenne et al., in press). In dicot plants such as Arabidopsis, iron uptake is based on a reduction strategy where iron(II) is taken-up by IRT1, whereas in grasses, it is based on iron(III) chelation by phytosiderophores (PS) in the rhizosphere prior PS-iron(III) uptake by roots (Hanikenne et al., in press; Kobayashi & Nishizawa, 2012). The chelation strategy provides higher uptake specificity and possibly enables less interference by divalent cations such as zinc, although PS were shown to bind zinc in the rhizosphere (Suzuki et al., 2006). None of the genes involved in the chelation strategy in grasses were among zinc-regulated genes in Brachypodium (Data S2). IRT1 homologs are also found in grasses (Evens et al., 2017) and were shown to transport zinc and iron (Ishimaru et al., 2006; Lee & An, 2009; Li et al., 2015). In this study, and in contrast to *OsIRT1* (Ishimaru et al., 2008), *BdIRT1* was regulated by zinc availability (Fig. S6). With other ZIPs sharing a similar expression pattern, *BdIRT1* may be involved in iron and zinc transport, and be responsible for higher accumulation of iron upon zinc deficiency (Fig. S2A), as well as for the parallel increase of zinc and iron uptake at early time-points upon zinc resupply (Fig. 5A-B).

Competition in root uptake between zinc and manganese/copper was possibly regulated by the same (or another set of) ZIP transporters (Fig. S2C,E). In rice and wheat, similar competition was reported

for manganese (Evens et al., 2017; Ishimaru et al., 2008). ZIP, as well as MTP, proteins can indeed potentially transport zinc and manganese (Milner et al., 2013). *AtMTP8* and *OsMTP8.1*, although responding to zinc deficiency, are manganese transporters (Chen et al., 2013; Chu et al., 2017). *BdHMA1*, homolog of *AtHMA1* (Kim et al., 2009; Seigneurin-Berny et al., 2006), a RootZIP cluster gene (Fig. 8), may mediate zinc/copper interactions. Moreover, among the metal homeostasis genes regulated by zinc in Brachypodium (Table 1, Fig. S5), seven are reported to encode proteins related to the human ATOX1 metallochaperone involved in copper chelation (Walker et al., 2002). Annotated as heavy-metal-associated domain (HMAD) containing proteins, these proteins are also known as heavy metal associated isoprenylated plant protein (*HIPP*) genes in plants (de Abreu-Neto et al., 2013). Arabidopsis and rice HIPP homologs were found to be cadmium-responsive and/or involved in copper transport (Shin et al., 2012; Zhang et al., 2018). Representing almost a quarter of metal homeostasis DEGs in our dataset (7/27), ATOX1-related copper chaperones may also be involved in zinc chelation in Brachypodium, indicating a complex metal interplay.

Transcriptional regulation of the Brachypodium zinc response

The AtbZIP19 and AtbZIP23 transcription factors from Arabidopsis are the best studied regulation system coordinating the zinc deficiency response in plants (Assunção et al., 2010). Homologs with conserved functions were characterized in barley, wheat and rice (Castro et al., 2017; Evens et al., 2017; Lilay et al., 2020; Nazri et al., 2017). The Brachypodium homolog of *AtbZIP19*, Bradi1g30140 [annotated as *BdbZIP9* in Phytozome v.12.1, but as *BdbZIP10* or *BdbZIP11* in (Glover-Cutter et al., 2014) or (Evens et al., 2017)] was previously suggested to be involved in a zinc deficiency-induced oxidative stress response (Glover-Cutter et al., 2014; Martin et al., 2018). However, here, *BdbZIP9* was barely regulated by zinc supply: it was slightly more expressed in zinc-deficient shoots compared to control plants and displayed a very flattened V-shape dynamics upon zinc resupply (Fig. S10A). AtbZIP19 and AtbZIP23 are proposed to be specialized in either roots or shoots, respectively (Arsova et al., 2019; Sinclair et al., 2018). *BdbZIP9* was more expressed in shoots than roots (Fig. S10A). Interestingly,

another *bZIP* gene, Bradi1g29920 (*BdbZIP8* in Phytozome v.12.1), was majorly expressed in roots (Fig. S10B) and, although it was not present among initially identified DEG (1.9-fold down-regulation 10 min after resupply, Data S1), it displayed the same V-shape expression pattern as ZIP cluster genes upon zinc resupply, suggesting that BdbZIP8 may be involved in zinc homeostasis in Brachypodium.

Additionally, 113 TFs from various families such as WRKY (25 genes), AP2 (24 genes), MYB (22 genes), bHLH (11 genes), and bZIP (9 genes) were among identified DEG (Data S7). None of them are homologs of known zinc regulatory genes and constitute new candidates for a role in zinc homeostasis regulation in grasses.

Zinc translocation to the shoot is a slow process

Zinc translocation to shoots was delayed relative to the rapid zinc re-entry in root tissues upon zinc resupply in Brachypodium, similar to earlier observations in Arabidopsis (Arsova et al., 2019). The Arabidopsis AtHMA2 and AtHMA4 pumps, as well as their rice homolog OsHMA2 were shown to be mostly responsible for root-to-shoot zinc transfer (Hussain et al., 2004; Satoh-Nagasawa et al., 2012). Whereas *AtHMA2* expression is induced by zinc deficiency (Arsova et al., 2019; Sinclair et al., 2018), *AtHMA4* and *OsHMA2* expression is barely regulated by zinc (Talke et al., 2006; Wintz et al., 2003; Yamada et al., 2013). Their Brachypodium homolog (Bradi1g34140) was moderately induced by zinc deficiency (1.6 fold) in roots, then transiently down-regulated upon zinc resupply before peaking at after 8 h (Fig. S10C). This up-regulation may be responsible for zinc re-entry observed in shoots after 5 h of resupply (Fig. 10), based on modelling showing that small variations in *HMA4* expression in Arabidopsis suffice to produce large effects in zinc efflux of symplast and to vasculature (Claus et al., 2013). The Bradi1g34140 late induction upon zinc resupply may therefore be responsible for delayed zinc accumulation in shoots. Moreover, the *PCR11*-related gene, found among zinc-responsive genes in Brachypodium (Table 1) was up-regulated at the 10 min and 30 min resupply time-points and gradually down-regulated thereafter (Fig. S6, Cluster #7). It may serve as a minimal shoot zinc supplier when the HMA pump is down-regulated (Song et al., 2010).

In contrast to zinc, copper and manganese concentrations changed quickly upon zinc resupply. Both metals experienced an increase at 10 min and then a decrease at 30 min, the inverse of the V-shape of ZIP clusters in root and shoot, although it was only significant in root (Fig. 5C-D). *OsNRAMP5* is suggested to function in manganese distribution from root into shoot (Yang et al., 2014). The zinc-responsive *NRAMP* gene (homolog of *OsNRAMP6, Bradi1g53150*) may serve the same function in Brachypodium. Its severe induction at 10 min time-point and with excess zinc, where manganese concentration is lowered (Fig. S10D) can support its role in manganese root-to-shoot translocation. On the other hand, *OsATX1*, homolog of *ATOX1*-related copper chaperone, was reported to have an important role in root-to-shoot copper translocation (Zhang et al., 2018) and to interact with multiple rice HMA pumps, probably to transfer copper to these pumps. There are seven *ATOX1*-related genes in the metal list, some of which were immediately regulated by zinc resupply (Clusters #4 in Fig. S6, cluster #8 in Fig. S7). Rapid induction of the *NRAMP* gene and several *ATOX1*-related genes (Fig. S5), in contrast to the late induction of *AtHMA4* homolog (Bradi1g34140), might explain the efficient regulation of manganese and copper concentration in shoot, compared to zinc.

Zinc shock appears to be the first transcriptomics response upon Zn resupply to deficient roots

Expression patterns of the root ZIP cluster genes (Fig. 8 and 9) were in stark contrast to observations made in Arabidopsis. In Brachypodium, genes within this cluster were highly expressed at zinc deficiency, rapidly down-regulated after 10 min resupply, then up again after 30 min, thus displaying a V-shape expression pattern (Fig. 8 and 9). This response occurred in roots as zinc concentration was steadily increasing upon resupply (Fig. 5A and 10A). In Arabidopsis was observed an initial up-regulation in roots of multiple metal homeostasis genes and proteins, including ZIPs, after 10 min of resupply of zinc-starved plant before a down-regulation from 30 min (Arsova et al., 2019).

The V-shape expression pattern of the ZIP cluster genes in roots implies that zinc influx into roots of zinc-starved plants is sensed as a zinc stress, similar to a zinc excess. This sensing then initiates within 10 minutes down-regulation of zinc uptake genes in roots. Such zinc shock response was described in

509 the yeast *Saccharomyces cerevisiae* (MacDiarmid et al., 2003; Simm et al., 2007). Thereafter, upon
510 sensing yet below-sufficient zinc levels in root tissues, *ZIP* genes are re-up-regulated at 30 minutes
511 followed by more classical down-regulation with increasing zinc concentrations in tissues at later time-
512 points. The response to zinc resupply in roots therefore occurs in two phases (Fig. 6A,D), an initial and
513 rapid phase (10-30 minutes) combining zinc shock response as well as zinc reuptake supported by
514 intense signaling (Fig. 7A), and a later phase (2-8 hours) which corresponds to a slow return to a
515 sufficient state. Although they display very different dynamics, two phases are also observed in
516 response to zinc resupply in Arabidopsis (Arsova et al., 2019).

517

518 **Early transcriptomic response of zinc transporter genes in shoots mirrors the root pattern and is**
519 **independent of local zinc concentration**

520 Strikingly, shoot ZIP cluster genes (Fig. 8 and 9) displayed a V-shape expression pattern as in roots (Fig.
521 8 and 10) although no change in shoot zinc level can be detected within this time-frame (Fig. 5A and
522 10B). In Arabidopsis no regulation of ZIPs at transcriptional or translational level was observed in
523 shoots before 8 h of zinc resupply (Arsova et al., 2019). Thus, early transcriptomic response of zinc
524 transporter genes in shoots appears to be independent of local zinc concentration and to be
525 coordinated with roots in Brachypodium and we propose that zinc re-entry in roots initiates a root-to-
526 shoot signaling that instigates a distant transcriptomic response (Fig. 11).

527 Shoot transcriptome response, independent from shoot nutrient concentration, was reported upon
528 nitrogen resupply to nitrogen-starved maize plants (Takei et al., 2002). In roots, several signaling-
529 related BPs were enriched at 10 min and 30 min time-points (Fig. 7A, dense red area, up-regulated
530 genes), while this response was delayed in shoots where metal transport (Fig. 7B, in blue, down-
531 regulated genes) was among the few enriched BPs after 10 min (Fig. 7B). It is therefore tempting to
532 speculate that the root-to-shoot signaling directly represses expression of metal transporter genes in
533 shoot, rather than activating local signaling pathways in shoot. Supporting this idea is that the “RNA

534 metabolism" BP was also enriched (Fig. 7B, in red, up-regulated genes), 10 min after resupply in shoots.
535 Several transcription factors were found in this enriched BP, and belong to different superfamilies such
536 as B3, AP2, WRKY and bZIP (Bradi4g02570, Data S3). These TFs may potentially regulate *ZIP* genes in
537 Brachypodium shoots upon zinc resupply.

538 Long-distance signaling mechanisms known in plants include electric or hydraulic signaling, calcium
539 waves propagated by calcium-dependent protein kinases and calmoduline proteins, ROS waves, sugar
540 signaling, hormonal signaling and mobile mRNA (Shabala et al., 2016). Among the signaling-related
541 DEG and enriched BPs at 10 min in root, multiple genes connected to these processes are present and
542 constitute candidates for producing root-to-shoot signals (Data S5).

543 Long distance or systemic signaling is known to contribute to metal homeostasis regulation. It was
544 suggested that *AtMTP2* and *AtHMA2* transcript levels in roots are regulated by shoot zinc
545 concentration in Arabidopsis, in contrast to *ZIP* genes being controlled by the local zinc status (Sinclair
546 et al., 2018). Designing an experiment testing our model of root-to-shoot signaling upon nutrient
547 resupply is a challenge. Split-root experiments were successful to disentangle local versus systemic
548 signals regulating the response to iron deficiency (Schikora & Schmidt, 2001; Vert et al., 2003; Wang
549 et al., 2007). To study systemic shoot-to-root signaling, reciprocal grafting of mutant and wild-type
550 roots and shoots, and foliar nutrient supply are popular methods (Sinclair et al., 2018; Tsutsui et al.,
551 2020). Conversely, treating half of the root system with deficient medium allows detecting a shoot
552 deficiency response while still sufficiently supplied by the other half of the root, and thus characterizing
553 a root-to-shoot deficiency signal. In the case of a long-distance signal triggered upon resupply of
554 deficient plants, it is delicate to distinguish signaling from delayed nutrient flux in such experimental
555 setups and alternative approaches will need to be designed to identify the putative signal.

556 In summary, our study revealed the complexity of the zinc homeostasis network in Brachypodium by
557 comparing static and dynamic responses to zinc supply. We identified a short-lived zinc shock response
558 to zinc resupply in roots and hypothetical long-distance zinc signaling that could be important in

559 realistic field resupply conditions. The study also showed that Brachypodium responds phenotypically
560 and genetically to changes in zinc supply, and represents a valuable model of staple grass crops to
561 examine zinc homeostasis that contrasts with the widely studied model Arabidopsis. Differences in
562 zinc/iron interactions and in dynamics of transcriptional changes upon zinc resupply reveal the
563 diversity of zinc homeostasis mechanisms among plant species.

564 **Acknowledgements**

565 Funding was provided by F.R.S.-FNRS grants MIS F.4511.16, CDR J.0009.17 and PDR T0120.18 (MH).
566 Marie Schloesser, Marie Scheuren, Cédric Delforge, Ana Galinski, Berndt Kastenholz, and Tanja Ehrlich
567 are thanked for technical assistance. The GIGA Genomics platform (ULiege) and the Durandal cluster
568 (InBioS-PhytoSystems, ULiege) are thanked for access to sequencing and computational resources,
569 respectively. SA is funded by a PhD grant of FZJ. MH is a Senior Research Associate of F.R.S.-FNRS. No
570 conflict of interest.

571 **Author contributions**

572 MH, SA and BA designed the research. SA performed experiments. SA, MH, BA analyzed the data. SG,
573 MC, BB and PM contributed to data interpretation. SA made the figures. SA, MH and BA wrote the
574 manuscript with contributions by MW. All authors read and approved the manuscript.

575 **References**

576 Alloway, B. J. (2008). Micronutrients and Crop Production: An Introduction. In B. J. Alloway (Ed.),
577 *Micronutrient Deficiencies in Global Crop Production* (pp. 1-39). Dordrecht: Springer
578 Netherlands.
579 Anders, S., Pyl, P. T., & Huber, W. (2014). HTSeq—a Python framework to work with high-throughput
580 sequencing data. *Bioinformatics, 31*(2), 166-169. doi:10.1093/bioinformatics/btu638
581 Arsova, B., Amini, S., Scheepers, M., Baiwir, D., Mazzucchelli, G., Carnol, M., et al. (2019). Resolution
582 of the proteome, transcript and ionome dynamics upon Zn re-supply in Zn-deficient
583 Arabidopsis. *bioRxiv*, 600569. doi:10.1101/600569

584 Assunção, A. G., Herrero, E., Lin, Y. F., Huettel, B., Talukdar, S., Smaczniak, C., et al. (2010). Arabidopsis
585 thaliana transcription factors bZIP19 and bZIP23 regulate the adaptation to zinc deficiency.
586 *Proc Natl Acad Sci U S A, 107*(22), 10296-10301.
587 Assunção, A. G. L., Persson, D. P., Husted, S., Schjørring, J. K., Alexander, R. D., & Aarts, M. G. M. (2013).
588 Model of how plants sense zinc deficiency. *Metallomics, 5*(9), 1110-1116.
589 doi:10.1039/C3MT00070B
590 Bandyopadhyay, T., Mehra, P., Hairat, S., & Giri, J. (2017). Morpho-physiological and transcriptome
591 profiling reveal novel zinc deficiency-responsive genes in rice. *Functional and Integrative*
592 *Genomics, 17*(5), 565-581. doi:10.1007/s10142-017-0556-x
593 Baxter, I., Tchieu, J., Sussman, M. R., Boutry, M., Palmgren, M. G., Gribskov, M., et al. (2003). Genomic
594 comparison of P-type ATPase ion pumps in Arabidopsis and rice. *Plant Physiol, 132*(2), 618-
595 628.
596 Benedicto, A., Hernández-Apaolaza, L., Rivas, I., & Lucena, J. J. (2011). Determination of 67Zn
597 distribution in navy bean (Phaseolus vulgaris L.) after foliar application of 67Zn-lignosulfonates
598 using isotope pattern deconvolution. *J Agric Food Chem, 59*(16), 8829-8838.
599 doi:10.1021/jf2002574
600 Bolger, A. M., Lohse, M., & Usadel, B. (2014). Trimmomatic: a flexible trimmer for Illumina sequence
601 data. *Bioinformatics, 30*(15), 2114-2120. doi:10.1093/bioinformatics/btu170
602 Brkljacic, J., Grotewold, E., Scholl, R., Mockler, T., Garvin, D. F., Vain, P., et al. (2011). Brachypodium as
603 a Model for the Grasses: Today and the Future. *Plant Physiology, 157*(1), 3-13.
604 doi:10.1104/pp.111.179531
605 Broadley, M. R., White, P. J., Hammond, J. P., Zelko, I., & Lux, A. (2007). Zinc in plants. *New Phytol,*
606 *173*(4), 677-702.
607 Castro, P. H., Lilay, G. H., Munõz-Mérida, A., Schjoerring, J. K., Azevedo, H., & Assuncąõ, A. G. L. (2017).
608 Phylogenetic analysis of F-bZIP transcription factors indicates conservation of the zinc
609 deficiency response across land plants. *Scientific Reports, 7*(1). doi:10.1038/s41598-017-
610 03903-6
611 Chaney, R. L. (1993). Zinc Phytotoxicity. In A. D. Robson (Ed.), *Zinc in Soils and Plants: Proceedings of*
612 *the International Symposium on 'Zinc in Soils and Plants' held at The University of Western*
613 *Australia, 27–28 September, 1993* (pp. 135-150). Dordrecht: Springer Netherlands.
614 Chen, X., & Ludewig, U. (2018). Biomass increase under zinc deficiency caused by delay of early
615 flowering in Arabidopsis. *Journal of Experimental Botany, 69*(5), 1269-1279.
616 doi:10.1093/jxb/erx478

617 Chen, Z., Fujii, Y., Yamaji, N., Masuda, S., Takemoto, Y., Kamiya, T., et al. (2013). Mn tolerance in rice is
618 mediated by MTP8. 1, a member of the cation diffusion facilitator family. *Journal of*
619 *Experimental Botany, 64*, 4375-4387.
620 Chochois, V., Voge, J. P., Rebetzke, G. J., & Watt, M. (2015). Variation in adult plant phenotypes and
621 partitioning among seed and stem-borne roots across Brachypodium distachyon accessions to
622 exploit in breeding cereals for well-watered and drought environments. *Plant Physiology,*
623 *168*(3), 953-967. doi:10.1104/pp.15.00095
624 Choi, S., & Bird, A. J. (2014). Zinc'ing sensibly: controlling zinc homeostasis at the transcriptional level.
625 *Metallomics, 6*(7), 1198-1215. doi:10.1039/C4MT00064A
626 Chu, H.-H., Car, S., Socha, A. L., Hindt, M. N., Punshon, T., & Guerinot, M. L. (2017). The Arabidopsis
627 MTP8 transporter determines the localization of manganese and iron in seeds. *Scientific*
628 *Reports, 7*(1), 11024. doi:10.1038/s41598-017-11250-9
629 Claus, J., Bohmann, A., & Chavarría-Krauser, A. (2013). Zinc uptake and radial transport in roots of
630 *Arabidopsis thaliana*: a modelling approach to understand accumulation. *Annals of Botany,*
631 *112*, 369-380. doi:10.1093/aob/mcs263
632 Clemens, S., Palmgren, M. G., & Kramer, U. (2002). A long way ahead: understanding and engineering
633 plant metal accumulation. *Trends Plant Sci, 7*(7), 309-315.
634 Colangelo, E. P., & Guerinot, M. L. (2006). Put the metal to the petal: metal uptake and transport
635 throughout plants. *Curr Opin Plant Biol, 9*(3), 322-330.
636 de Abreu-Neto, J. B., Turchetto-Zolet, A. C., de Oliveira, L. F. V., Bodanese Zanettini, M. H., & Margis-
637 Pinheiro, M. (2013). Heavy metal-associated isoprenylated plant protein (HIPP):
638 characterization of a family of proteins exclusive to plants. *FEBS Journal, 280*(7), 1604-1616.
639 doi:10.1111/febs.12159
640 Durand, E., Bouchet, S., Bertin, P., Ressayre, A., Jamin, P., Charcosset, A., et al. (2012). Flowering time
641 in maize: Linkage and epistasis at a major effect locus. *Genetics, 190*(4), 1547-1562.
642 doi:10.1534/genetics.111.136903
643 Evens, N. P., Buchner, P., Williams, L. E., & Hawkesford, M. J. (2017). The role of ZIP transporters and
644 group F bZIP transcription factors in the Zn-deficiency response of wheat (Triticum aestivum).
645 *The Plant Journal, 92*(2), 291-304. doi:doi:10.1111/tpj.13655
646 Fukao, Y., Ferjani, A., Tomioka, R., Nagasaki, N., Kurata, R., Nishimori, Y., et al. (2011). iTRAQ Analysis
647 Reveals Mechanisms of Growth Defects Due to Excess Zinc in Arabidopsis. *Plant Physiol,*
648 *155*(4), 1893-1907.
649 Glover-Cutter, K. M., Alderman, S., Dombrowski, J. E., & Martin, R. C. (2014). Enhanced Oxidative Stress
650 Resistance through Activation of a Zinc Deficiency Transcription Factor in Brachypodium
651 Distachyon. *Plant Physiology, 166*(3), 1492-1505. doi:10.1104/pp.114.240457

652 Gupta, N., Ram, H., & Kumar, B. (2016). Mechanism of Zinc absorption in plants: uptake, transport,
653 translocation and accumulation. *Reviews in Environmental Science and Bio/Technology, 15*(1),
654 89-109. doi:10.1007/s11157-016-9390-1
655 Hall, J. L., & Williams, L. E. (2003). Transition metal transporters in plants. *J Exp Bot, 54*(393), 2601-
656 2613.
657 Hanikenne, M., Esteves, S. M., Fanara, S., & Rouached, H. (in press). An iron game: coordinated
658 homeostasis of essential nutrients. *J Exp Bot*.
659 Hong, S. Y., Seo, P. J., Yang, M. S., Xiang, F., & Park, C. M. (2008). Exploring valid reference genes for
660 gene expression studies in Brachypodium distachyon by real-time PCR. *BMC Plant Biology,*
661 *8*(1), 1-11. doi:10.1186/1471-2229-8-112
662 Howe, E. A., Sinha, R., Schlauch, D., & Quackenbush, J. (2011). RNA-Seq analysis in MeV. *Bioinformatics,*
663 *27*(22), 3209-3210. doi:10.1093/bioinformatics/btr490
664 Hu, W., Coomer, T. D., Loka, D. A., Oosterhuis, D. M., & Zhou, Z. (2017). Potassium deficiency affects
665 the carbon-nitrogen balance in cotton leaves. *Plant Physiology and Biochemistry, 115*, 408-
666 417. doi:10.1016/j.plaphy.2017.04.005
667 Huang, S., Sasaki, A., Yamaji, N., Okada, H., Mitani-Ueno, N., & Ma, J. F. (2020). The ZIP transporter
668 family member OsZIP9 contributes to root zinc uptake in rice under zinc-limited conditions.
669 *Plant Physiology, 183*(3), 1224-1234. doi:10.1104/pp.20.00125
670 Hussain, D., Haydon, M. J., Wang, Y., Wong, E., Sherson, S. M., Young, J., et al. (2004). P-type ATPase
671 heavy metal transporters with roles in essential zinc homeostasis in Arabidopsis. *Plant Cell,*
672 *16*(5), 1327-1339.
673 Ishimaru, Y., Suzuki, M., Kobayashi, T., Takahashi, M., Nakanishi, H., Mori, S., et al. (2005). OsZIP4, a
674 novel zinc-regulated zinc transporter in rice. *J Exp Bot, 56*(422), 3207-3214.
675 Ishimaru, Y., Suzuki, M., Ogo, Y., Takahashi, M., Nakanishi, H., Mori, S., et al. (2008). Synthesis of
676 nicotianamine and deoxymugineic acid is regulated by OsIRO2 in Zn excess rice plants. *Soil*
677 *Science and Plant Nutrition, 54*(3), 417-423. doi:10.1111/j.1747-0765.2008.00259.x
678 Ishimaru, Y., Suzuki, M., Tsukamoto, T., Suzuki, K., Nakazono, M., Kobayashi, T., et al. (2006). Rice plants
679 take up iron as an Fe^{3+}-phytosiderophore and as Fe^{2+}. *Plant J, 45*(3), 335-346.
680 Jensen, J., & Pedersen, M. B. (2006). Ecological risk assessment of contaminated soil. *Rev Environ*
681 *Contam Toxicol, 186*, 73-105. doi:10.1007/0-387-32883-1_3
682 Jung, H. I., Gayomba, S. R., Yan, J., & Vatamaniuk, O. K. (2014). Brachypodium distachyon as a model
683 system for studies of copper transport in cereal crops. *Frontiers in Plant Science, 5*(MAY).
684 doi:10.3389/fpls.2014.00236

685 Kavitha, P. G., Kuruvilla, S., & Mathew, M. K. (2015). Functional characterization of a transition metal
686 ion transporter, OsZIP6 from rice (*Oryza sativa* L.). *Plant Physiology and Biochemistry, 97*, 165-
687 174. doi:http://dx.doi.org/10.1016/j.plaphy.2015.10.005
688 Kim, Y. Y., Choi, H., Segami, S., Cho, H. T., Martinoia, E., Maeshima, M., et al. (2009). AtHMA1
689 contributes to the detoxification of excess Zn(II) in Arabidopsis. *Plant J, 58*, 737-753.
690 Klatte, M., Schuler, M., Wirtz, M., Fink-Straube, C., Hell, R., & Bauer, P. (2009). The analysis of
691 Arabidopsis nicotianamine synthase mutants reveals functions for nicotianamine in seed iron
692 loading and iron deficiency responses. *Plant Physiol, 150*(1), 257-271.
693 Kobayashi, T., & Nishizawa, N. K. (2012). Iron Uptake, Translocation, and Regulation in Higher Plants.
694 *Annu Rev Plant Biol, 63*(1), 131-152. doi:doi:10.1146/annurev-arplant-042811-105522
695 Kolář, J., & Seňková, J. (2008). Reduction of mineral nutrient availability accelerates flowering of
696 Arabidopsis thaliana. *Journal of Plant Physiology, 165*(15), 1601-1609.
697 doi:10.1016/j.jplph.2007.11.010
698 Krämer, U. (2010). Metal hyperaccumulation in plants. *Annu Rev Plant Biol, 61*, 517-534.
699 Krämer, U., Talke, I. N., & Hanikenne, M. (2007). Transition metal transport. *FEBS Lett, 581*, 2263-2272.
700 Lee, S., & An, G. (2009). Over-expression of OsIRT1 leads to increased iron and zinc accumulations in
701 rice. *Plant, Cell & Environment, 32*(4), 408-416. doi:10.1111/j.1365-3040.2009.01935.x
702 Lee, S., Jeong, H. J., Kim, S. A., Lee, J., Guerinot, M. L., & An, G. (2010). OsZIP5 is a plasma membrane
703 zinc transporter in rice. *Plant Mol Biol, 73*(4-5), 507-517.
704 Lešková, A., Giehl, R. F. H., Hartmann, A., Fargašová, A., & von Wirén, N. (2017). Heavy Metals Induce
705 Iron Deficiency Responses at Different Hierarchic and Regulatory Levels. *Plant Physiology,*
706 *174*(3), 1648-1668. doi:10.1104/pp.16.01916
707 Li, S., Zhou, X., Li, H., Liu, Y., Zhu, L., Guo, J., et al. (2015). Overexpression of ZmIRT1 and ZmZIP3
708 Enhances Iron and Zinc Accumulation in Transgenic Arabidopsis. *PLoS ONE, 10*(8), e0136647-
709 e0136647. doi:10.1371/journal.pone.0136647
710 Li, S., Zhou, X., Zhao, Y., Li, H., Liu, Y., Zhu, L., et al. (2016). Constitutive expression of the ZmZIP7 in
711 Arabidopsis alters metal homeostasis and increases Fe and Zn content. *Plant Physiology and*
712 *Biochemistry, 106*, 1-10. doi:10.1016/j.plaphy.2016.04.044
713 Lilay, G. H., Castro, P. H., Campilho, A., & Assunção, A. G. L. (2019). The Arabidopsis bZIP19 and bZIP23
714 Activity Requires Zinc Deficiency – Insight on Regulation From Complementation Lines.
715 *Frontiers in Plant Science, 9*. doi:10.3389/fpls.2018.01955
716 Lilay, G. H., Castro, P. H., Guedes, J. G., Almeida, D. M., Campilho, A., Azevedo, H., et al. (2020). Rice F-
717 bZIP transcription factors regulate the zinc deficiency response. *Journal of Experimental*
718 *Botany, 71*(12), 3664-3677. doi:10.1093/jxb/eraa115

719 Liu, Z., Giehl, R. F. H., Hartmann, A., Hajirezaei, M. R., Carpentier, S., & von Wirén, N. (2020). Seminal
720 and Nodal Roots of Barley Differ in Anatomy, Proteome and Nitrate Uptake Capacity. *Plant &*
721 *cell physiology, 61*(7), 1297-1308. doi:10.1093/pcp/pcaa059
722 Love, M. I., Huber, W., & Anders, S. (2014). Moderated estimation of fold change and dispersion for
723 RNA-seq data with DESeq2. *Genome Biology, 15*(12), 550. doi:10.1186/s13059-014-0550-8
724 MacDiarmid, C. W., Milanick, M. A., & Eide, D. J. (2003). Induction of the ZRC1 metal tolerance gene in
725 zinc-limited yeast confers resistance to zinc shock. *J Biol Chem, 278*(17), 15065-15072.
726 MacFarlane, G. R., & Burchett, M. D. (2002). Toxicity, growth and accumulation relationships of copper,
727 lead and zinc in the grey mangrove Avicennia marina (Forsk.) Vierh. *Marine Environmental*
728 *Research, 54*(1), 65-84. doi:10.1016/S0141-1136(02)00095-8
729 Marschner, H., Römheld, V., & Kissel, M. (1986). Different strategies in higher plants in mobilization
730 and uptake of iron. *Journal of Plant Nutrition, 9*(3-7), 695-713.
731 doi:10.1080/01904168609363475
732 Martin, R. C., Vining, K., & Dombrowski, J. E. (2018). Genome-wide (ChIP-seq) identification of target
733 genes regulated by BdbZIP10 during paraquat-induced oxidative stress. *BMC Plant Biology,*
734 *18*(1). doi:10.1186/s12870-018-1275-8
735 Milner, M. J., Seamon, J., Craft, E., & Kochian, L. V. (2013). Transport properties of members of the ZIP
736 family in plants and their role in Zn and Mn homeostasis. *Journal of Experimental Botany, 64*(1),
737 369-381. doi:10.1093/jxb/ers315
738 Nagel, K. A., Kastenholz, B., Jahnke, S., van Dusschoten, D., Aach, T., Mühlich, M., et al. (2009).
739 Temperature responses of roots: impact on growth, root system architecture and implications
740 for phenotyping. *Functional Plant Biology, 36*(11), 947-947. doi:10.1071/FP09184
741 Nazri, A. Z., Griffin, J. H. C., Peaston, K. A., Alexander-Webber, D. G. A., & Williams, L. E. (2017). F-group
742 bZIPs in barley – a role in Zn deficiency. *Plant, Cell & Environment, 40*, 2754–2770.
743 doi:10.1111/pce.13045
744 Nouet, C., Charlier, J. B., Carnol, M., Bosman, B., Farnir, F., Motte, P., et al. (2015). Functional analysis
745 of the three *HMA4* copies of the metal hyperaccumulator *Arabidopsis halleri*. *J Exp Bot, 66*(19),
746 5783-5795. doi:10.1093/jxb/erv280
747 Pertea, M., Kim, D., Pertea, G. M., Leek, J. T., & Salzberg, S. L. (2016). Transcript-level expression
748 analysis of RNA-seq experiments with HISAT, StringTie and Ballgown. *Nature Protocols, 11*(9),
749 1650-1667. doi:10.1038/nprot.2016.095
750 Pineau, C., Loubet, S., Lefoulon, C., Chalies, C., Fizames, C., Lacombe, B., et al. (2012). Natural Variation
751 at the *FRD3* MATE Transporter Locus Reveals Cross-Talk between Fe Homeostasis and Zn
752 Tolerance in *Arabidopsis thaliana*. *PLoS Genet, 8*(12), e1003120.
753 doi:10.1371/journal.pgen.1003120

754 Poiré, R., Chochois, V., Sirault, X. R. R., Vogel, J. P., Watt, M., & Furbank, R. T. (2014). Digital imaging
755 approaches for phenotyping whole plant nitrogen and phosphorus response in Brachypodium
756 distachyon. *Journal of Integrative Plant Biology, 56*(8), 781-796. doi:10.1111/jipb.12198
757 Ramesh, S. A., Shin, R., Eide, D. J., & Schachtman, D. P. (2003). Differential metal selectivity and gene
758 expression of two zinc transporters from rice. *Plant Physiology, 133*(1), 126-134.
759 doi:10.1104/pp.103.026815
760 Raudvere, U., Kolberg, L., Kuzmin, I., Arak, T., Adler, P., Peterson, H., et al. (2019). g:Profiler: a web
761 server for functional enrichment analysis and conversions of gene lists (2019 update). *Nucleic*
762 *Acids Research, 47*(W1), W191-W198. doi:10.1093/nar/gkz369
763 Ricachenevsky, F. K., Menguer, P. K., Sperotto, R. A., & Fett, J. P. (2015). Got to hide your Zn away:
764 Molecular control of Zn accumulation and biotechnological applications. *Plant Science, 236*, 1-
765 17. doi:https://doi.org/10.1016/j.plantsci.2015.03.009
766 Ricachenevsky, F. K., Sperotto, R. A., Menguer, P. K., Sperb, E. R., Lopes, K. L., & Fett, J. P. (2011). ZINC-
767 INDUCED FACILITATOR-LIKE family in plants: lineage-specific expansion in monocotyledons
768 and conserved genomic and expression features among rice (Oryza sativa) paralogs. *BMC Plant*
769 *Biology, 11*(1), 20. doi:10.1186/1471-2229-11-20
770 Saenchai, C., Bouain, N., Kisko, M., Prom-u-thai, C., Doumas, P., & Rouached, H. (2016). The
771 involvement of OsPHO1;1 in the regulation of iron transport through integration of phosphate
772 and zinc deficiency signalling. *Frontiers in Plant Science, 7*. doi:10.3389/fpls.2016.00396
773 Satoh-Nagasawa, N., Mori, M., Nakazawa, N., Kawamoto, T., Nagato, Y., Sakurai, K., et al. (2012).
774 Mutations in Rice (Oryza sativa) Heavy Metal ATPase 2 (OsHMA2) Restrict the Translocation of
775 Zinc and Cadmium. *Plant and Cell Physiology, 53*(1), 213-224. doi:10.1093/pcp/pcr166
776 Scheepers, M., Spielmann, J., Boulanger, M., Carnol, M., Bosman, B., De Pauw, E., et al. (2020).
777 Intertwined metal homeostasis, oxidative and biotic stress responses in the Arabidopsis *frd3*
778 mutant. *The Plant Journal, 102*, 34-52. doi:10.1111/tpj.14610
779 Schikora, A., & Schmidt, W. (2001). Iron stress-induced changes in root epidermal cell fate are
780 regulated independently from physiological responses to low iron availability. *Plant*
781 *Physiology, 125*(4), 1679-1687. doi:10.1104/pp.125.4.1679
782 Seigneurin-Berny, D., Gravot, A., Auroy, P., Mazard, C., Kraut, A., Finazzi, G., et al. (2006). HMA1, a new
783 Cu-ATPase of the chloroplast envelope, is essential for growth under adverse light conditions.
784 *J Biol Chem, 281*(5), 2882-2892.
785 Shabala, S., White, R. G., Djordjevic, M. A., Ruan, Y.-L., & Mathesius, U. (2016). Root-to-shoot signalling:
786 integration of diverse molecules, pathways and functions. *Functional Plant Biology, 43*(2), 87-
787 104. doi:https://doi.org/10.1071/FP15252

788 Shanmugam, V., Tsednee, M., & Yeh, K.-C. (2012). ZINC TOLERANCE INDUCED BY IRON 1 reveals the
789 importance of glutathione in the cross-homeostasis between zinc and iron in *Arabidopsis*
790 *thaliana*. *The Plant Journal, 69*(6), 1006-1017. doi:10.1111/j.1365-313X.2011.04850.x
791 Shin, L. J., Lo, J. C., & Yeh, K. C. (2012). Copper chaperone antioxidant Protein1 is essential for Copper
792 homeostasis. *Plant Physiology, 159*(3), 1099-1110. doi:10.1104/pp.112.195974
793 Shojima, S., Nishizawa, N. K., Fushiya, S., Nozoe, S., Irifune, T., & Mori, S. (1990). Biosynthesis of
794 phytosiderophores: In vitro biosynthesis of 2'-deoxymugineic acid from L-methionine and
795 nicotianamine. *Plant Physiology, 93*(4), 1497-1503. doi:10.1104/pp.93.4.1497
796 Simm, C., Lahner, B., Salt, D., LeFurgey, A., Ingram, P., Yandell, B., et al. (2007). *Saccharomyces*
797 *cerevisiae* vacuole in zinc storage and intracellular zinc distribution. *Eukaryotic Cell, 6*(7), 1166-
798 1177. doi:10.1128/EC.00077-07
799 Sinclair, S. A., & Krämer, U. (2012). The zinc homeostasis network of land plants. *Biochim Biophys Acta,*
800 *1823*, 1553-1567. doi:10.1016/j.bbamcr.2012.05.016
801 Sinclair, S. A., Senger, T., Talke, I. N., Cobbett, C. S., Haydon, M. J., & Kraemer, U. (2018). Systemic
802 upregulation of MTP2- and HMA2-mediated Zn partitioning to the shoot supplements local Zn
803 deficiency responses of Arabidopsis. *The Plant cell, 30*, 2463-2479. doi:10.1105/tpc.18.00207
804 Smith, D. D., Sperry, J. S., & Adler, F. R. (2017). Convergence in leaf size versus twig leaf area scaling:
805 do plants optimize leaf area partitioning? *Ann Bot., 119*(3), 447-456.
806 Song, W. Y., Choi, K. S., Kim, D. Y., Geisler, M., Park, J., Vincenzetti, V., et al. (2010). Arabidopsis PCR2
807 Is a Zinc Exporter Involved in Both Zinc Extrusion and Long-Distance Zinc Transport. *Plant Cell,*
808 *22*, 2237-2252.
809 Spielmann, J., Ahmadi, H., Scheepers, M., Weber, M., Nitsche, S., Carnol, M., et al. (2020). The two
810 copies of the zinc and cadmium ZIP6 transporter of *Arabidopsis halleri* have distinct effects on
811 cadmium tolerance. *Plant, Cell & Environment*. doi:10.1111/pce.13806
812 Steffens, B., & Rasmussen, A. (2016). The physiology of adventitious roots. *Plant Physiology, 170*(2),
813 603-617. doi:10.1104/pp.15.01360
814 Subedi, S. R., Sandhu, N., Singh, V. K., Sinha, P., Kumar, S., Singh, S. P., et al. (2019). Genome-wide
815 association study reveals significant genomic regions for improving yield, adaptability of rice
816 under dry direct seeded cultivation condition. *BMC Genomics, 20*(1), 471-471.
817 doi:10.1186/s12864-019-5840-9
818 Suzuki, M., Takahashi, M., Tsukamoto, T., Watanabe, S., Matsuhashi, S., Yazaki, J., et al. (2006).
819 Biosynthesis and secretion of mugineic acid family phytosiderophores in zinc-deficient barley.
820 *Plant J, 48*(1), 85-97.

821 Suzuki, M., Tsukamoto, T., Inoue, H., Watanabe, S., Matsuhashi, S., Takahashi, M., et al. (2008).
822 Deoxymugineic acid increases Zn translocation in Zn-deficient rice plants. *Plant Molecular*
823 *Biology, 66*(6), 609-617. doi:10.1007/s11103-008-9292-x
824 Takahashi, M., Yamaguchi, H., Nakanishi, H., Shioiri, T., Nishizawa, N. K., & Mori, S. (1999). Cloning two
825 genes for nicotianamine aminotransferase, a critical enzyme in iron acquisition (strategy II) in
826 graminaceous plants. *Plant Physiology, 121*(3), 947-956. doi:10.1104/pp.121.3.947
827 Takahashi, R., Ishimaru, Y., Shimo, H., Ogo, Y., Senoura, T., Nishizawa, N. K., et al. (2012). The OsHMA2
828 transporter is involved in root-to-shoot translocation of Zn and Cd in rice. *Plant Cell Environ,*
829 *35*(11), 1948-1957. doi:10.1111/j.1365-3040.2012.02527.x
830 Takei, K., Takahashi, T., Sugiyama, T., Yamaya, T., & Sakakibara, H. (2002). Multiple Routes
831 Communicating Nitrogen Availability From Roots to Shoots: A Signal Transduction Pathway
832 Mediated by Cytokinin. *Journal of Experimental Botany, 53*(370), 971–977.
833 doi:10.1093/JEXBOT/53.370.971
834 Talke, I. N., Hanikenne, M., & Krämer, U. (2006). Zinc-Dependent Global Transcriptional Control,
835 Transcriptional Deregulation, and Higher Gene Copy Number for Genes in Metal Homeostasis
836 of the Hyperaccumulator *Arabidopsis halleri*. *Plant Physiol, 142*(1), 148-167.
837 Tennant, D. (1976). Root growth of wheat. I. Early patterns of multiplication and extension of wheat
838 roots including effects of levels of nitrogen, phosphorus and potassium. *Australian Journal of*
839 *Agricultural Research, 27*(2), 183-183. doi:10.1071/ar9760183
840 Tiong, J., McDonald, G. K., Genc, Y., Pedas, P., Hayes, J. E., Toubia, J., et al. (2014). HvZIP7 mediates zinc
841 accumulation in barley (Hordeum vulgare) at moderately high zinc supply. *New Phytologist,*
842 *201*, 131-143. doi:10.1111/nph.12468
843 Tsutsui, H., Yanagisawa, N., Kawakatsu, Y., Ikematsu, S., Sawai, Y., Tabata, R., et al. (2020).
844 Micrografting device for testing systemic signaling in Arabidopsis. *The Plant Journal, 103*, 918-
845 929. doi:10.1111/tpj.14768
846 Vallee, B. L., & Falchuk, K. H. (1993). The biochemical basis of zinc physiology. *Physiological Reviews,*
847 *73*(1), 79-118. doi:10.1152/physrev.1993.73.1.79
848 Vert, G. A., Briat, J. F., & Curie, C. (2003). Dual regulation of the Arabidopsis high-affinity root iron
849 uptake system by local and long-distance signals. *Plant Physiology, 132*(2), 796-804.
850 doi:10.1104/pp.102.016089
851 Vogel, J. P., Garvin, D. F., Mockler, T. C., Schmutz, J., Rokhsar, D., Bevan, M. W., et al. (2010). Genome
852 sequencing and analysis of the model grass Brachypodium distachyon. *Nature, 463*(7282), 763-
853 768. doi:10.1038/nature08747

854 Von Wirén, N., Marschner, H., & Romheld, V. (1996). Roots of Iron-Efficient Maize also Absorb
855 Phytosiderophore-Chelated Zinc. *Plant Physiology, 111*(4), 1119-1125.
856 doi:10.1104/pp.111.4.1119
857 Walker, J. M., Tsivkovskii, R., & Lutsenko, S. (2002). Metallochaperone Atox1 transfers copper to the
858 NH2-terminal domain of the Wilson's disease protein and regulates its catalytic activity.
859 *Journal of Biological Chemistry, 277*(31), 27953-27959. doi:10.1074/jbc.M203845200
860 Wang, H. Y., Klatte, M., Jakoby, M., Baumlein, H., Weisshaar, B., & Bauer, P. (2007). Iron deficiency-
861 mediated stress regulation of four subgroup Ib BHLH genes in *Arabidopsis thaliana*. *Planta,*
862 *226*(4), 897-908.
863 Watt, M., Schneebeli, K., Dong, P., & Wilson, I. W. (2009). The shoot and root growth of Brachypodium
864 and its potential as a model for wheat and other cereal crops. *Functional Plant Biology, 36*(11),
865 960-960. doi:10.1071/FP09214
866 Wintz, H., Fox, T., Wu, Y. Y., Feng, V., Chen, W., Chang, H. S., et al. (2003). Expression Profiles of
867 Arabidopsis thaliana in Mineral Deficiencies Reveal Novel Transporters Involved in Metal
868 Homeostasis. *J Biol Chem, 278*(48), 47644-47653.
869 Yamada, K., Nagano, A. J., Nishina, M., Hara-Nishimura, I., & Nishimura, M. (2013). Identification of
870 Two Novel Endoplasmic Reticulum Body-Specific Integral Membrane Proteins. *Plant*
871 *Physiology, 161*(1), 108-120. doi:10.1104/pp.112.207654
872 Yang, M., Zhang, Y., Zhang, L., Hu, J., Zhang, X., Lu, K., et al. (2014). OsNRAMP5 contributes to
873 manganese translocation and distribution in rice shoots. *Journal of Experimental Botany,*
874 *65*(17), 4849-4861. doi:10.1093/jxb/eru259
875 Yang, X., Huang, J., Jiang, Y., & Zhang, H. S. (2009). Cloning and functional identification of two
876 members of the ZIP (Zrt, Irt-like protein) gene family in rice (Oryza sativa L.). *Molecular Biology*
877 *Reports, 36*(2), 281-287. doi:10.1007/s11033-007-9177-0
878 Yordem, B. K., Conte, S. S., Ma, J. F., Yokosho, K., Vasques, K. A., Gopalsamy, S. N., et al. (2011).
879 Brachypodium distachyon as a new model system for understanding iron homeostasis in
880 grasses: Phylogenetic and expression analysis of Yellow Stripe-Like (YSL) transporters. *Annals*
881 *of Botany, 108*(5), 821-833. doi:10.1093/aob/mcr200
882 Zargar, S. M., Kurata, R., Inaba, S., Oikawa, A., Fukui, R., Ogata, Y., et al. (2015). Quantitative proteomics
883 of Arabidopsis shoot microsomal proteins reveals a cross-talk between excess zinc and iron
884 deficiency. *Proteomics, 15*, 1196–1201. doi:10.1002/pmic.201400467
885 Zeng, H., Zhang, X., Ding, M., & Zhu, Y. (2019). Integrated analyses of miRNAome and transcriptome
886 reveal zinc deficiency responses in rice seedlings. *BMC Plant Biology, 19*(1).
887 doi:10.1186/s12870-019-2203-2

888 Zhang, Y., Chen, K., Zhao, F. J., Sun, C., Jin, C., Shi, Y., et al. (2018). OsATX1 interacts with heavy metal
889 P1B-type ATPases and affects copper transport and distribution. *Plant Physiology, 178*(1), 329-
890 344. doi:10.1104/pp.18.00425

891

Table 1. Metal homeostasis-related genes among DEG lists

Brachypodium				Arabidopsis		Rice	
Gene ID	Description	Tissue	Cluster #	Gene ID	Description	Gene ID	Description
Bradi1g53680	ZIP13	Root, Shoot	2, 4	AT2G32270	ZIP3	Os07g12890	ZIP8
Bradi2g22520	ZIP5	Root, Shoot	2, 4	AT2G32270	ZIP3	Os05g39560	ZIP5
Bradi2g22530	ZIP9	Root, Shoot	2, 4	AT2G32270	ZIP3	Os05g39540	ZIP9
Bradi3g17900	ZIP4	Root, Shoot	2, 4	AT3G12750	ZIP1	Os08g10630	ZIP4
Bradi2g33110	ZIP7	Root, Shoot	2, 4	AT2G30080	ZIP6	Os05g10940	ZIP7
Bradi1g37667	ZIP10	Root, Shoot	2, 4	AT1G60960	IRT3	Os06g37010	ZIP10
Bradi1g12860	IRT1	Root	2	AT4G19690	IRT1	Os03g46470	IRT1
Bradi5g21580	ZIP3	Root	2	AT3G12750	ZIP1	Os04g52310	ZIP3
Bradi4g26366	MFS	Root	5	AT5G13740	ZIF1	Os11g04104	MFS antiporter
Bradi4g43620	MFS	Shoot	1	—	—	Os12g03870	MFS antiporter
Bradi5g08250	—	Root	1	AT5G41000	YSL4	Os04g32050	YSL6
Bradi5g08260	—	Root	1	AT5G41000	YSL4	Os04g32050	YSL6
Bradi1g33347	HMA1	Root	2	AT4G37270	HMA1	Os06g47550	Cd/Zn-transporting ATPase
Bradi1g68950	Zn/Fe transporter	Root	3	AT3G58060	MTP8	Os03g12530	MTP8.1
Bradi4g29720	—	Root	2	AT2G01770	VIT1	Os09g23300	Integral membrane protein
Bradi1g17090	NAS	Root	8	AT5G04950	NAS1	Os07g48980	NAS3
Bradi1g53150	Fe/Mn transporter	Root	9	—	—	Os07g15460	NRAMP6
Bradi5g12456	PCR11-related	Root	7	—	—	—	—
Bradi2g43120	ABC transporter	Root	9	AT1G15520	ABCG40/PDR12	Os01g42380	ABCG36/PDR9
Bradi2g31261	ATX2-related	Root	3	—	—	—	—
Bradi5g04560	HIPP26	Shoot	8	AT5G66110	HIPP27	Os04g17100	HIPP42
Bradi3g55480	ATOX1-related	Root	4	—	—	Os02g57350	—
Bradi3g44820	ATOX1-related	Root	5	AT3G56240	Cu chaperone	—	—
Bradi5g12930	ATOX1-related	Root	4	AT4G05030	Copper transport protein family	—	—
Bradi5g25440	ATOX1-related	Root	4	—	—	Os04g57200	heavy metal transport/detoxification protein
Bradi3g27550	ATOX1-related	Root	3	AT2G36950	Heavy metal transport/detoxification superfamily protein	Os10g30450	HIPP35
Bradi5g12960	ATOX1-related	Root	4	—	—	Os04g39350	heavy-metal-associated domain containing protein

892 Note that among the 27 Brachypodium genes listed here, only *BdHMA1* and *BdHIPP26* have been
893 attributed names in the Phytozome database (https://phytozome.jgi.doe.gov/pz/portal.html). For The
894 nomenclature proposed in an available ZIP family phylogeny study (Evens *et al.*, 2017) was used where,
895 among the nine *ZIP* genes present in this list, all received the same numbering as their rice homologs,
896 except for *BdZIP13* which related to *OsZIP8*.

897

Figure 1. Brachypodium plants grown hydroponically in different zinc regimes for 3 weeks. (a) Shoot and (b) representative root images of plants exposed to zinc deficiency (0 µM Zn, left), control (1.5 µM Zn, center) or excess (20 µM Zn, right) conditions. Pictures are representative of multiple independent experiments. Scale bars are 2 cm.

Figure 2. Shoot phenotype of Brachypodium plants upon zinc deficiency and excess. Plants grown hydroponically were exposed for 3 weeks to zinc deficiency (0 µM Zn), control (1.5 µM Zn) or excess (20 µM Zn) conditions. (a) Shoot fresh and (b) dry weight. (c) Total leaf area. (a-c) Bars show mean values (+/- standard deviation) of 9-12 individual plants for each treatment. (d) Leaf number per plant. Box and whisker plot showing the median (hardline), interquartile (box), 1.5 interquartile (whiskers) and outliers (dots) of values from 12 individual plants for each treatment. Letters indicate statistical differences (p-value < 0.05) according to Student's T-test.

Figure 3. Root phenotypic measures of Brachypodium plants under three weeks of zinc treatments. Plants grown hydroponically were exposed for 3 weeks to zinc deficiency (0 µM Zn), control (1.5 µM Zn) or excess (20 µM Zn) conditions. (a) Root fresh weight, (b) root dry weight, (c) total root length and (d) primary and lateral root length. (a-d) Bars show mean values (+/- standard deviation) of 9-12 individual plants for each treatment. (e) Nodal root number per plant. Box and whisker plot showing the median (hardline), interquartile (box), 1.5 interquartile (whiskers) and outliers (dots) of values from 9 individual plants for each treatment. Letters indicate statistical differences (p-value < 0.05) according to Student's T-test.

Figure 4. Zinc accumulation in roots and shoots of Brachypodium upon zinc deficiency and excess. Plants grown hydroponically were exposed for 3 weeks to zinc deficiency (0 µM Zn), control (1.5 µM Zn) or excess (20 µM Zn) conditions. (a) Root and (b) shoot zinc concentrations. (c) Shoot to root zinc concentration ratio (Log). Bars show mean values (+/- standard deviation) of three biological replicates (3-4 plants each). Letters indicate statistical differences (p-value < 0.05) according to Student's T-test.

Figure 5. Ionome profiling of roots and shoots of Brachypodium upon zinc deficiency and re-supply. Plants grown hydroponically under zinc deficiency (0 µM Zn) for 3 weeks were resupplied with 1 µM Zn and samples were harvested after short time points (10 minutes to 8 hours). Root and shoot (a) zinc (Zn), (b) iron (Fe), (c) copper (Cu), and (d) manganese (Mn) concentrations. Bars show mean values (+/- standard deviation) of three biological replicates (3-4 plants each). Letters indicate statistical differences (p-value < 0.05) according to one-way ANOVA.

Figure 6. RNA sequencing analysis of the steady-state response to zinc deficiency and excess and the dynamic response to zinc deficiency and resupply in Brachypodium. Data are from three biological replicates (3-4 plants each) for each treatment. Principal Component Analysis (PCA) of (a) root and (b)

931 shoot expression data. PCA of root and shoot data together is presented in Fig. S4. (c) Number of
932 Differentially Expressed Genes (DEG) in 9 selected contrasts in roots (brown cells) and in shoots (green
933 cells). Growth conditions are annotated in central white cells and DEGs identified in a contrast between
934 2 conditions are annotated in the intersecting cell, with numbers of up- (left) and down- (right)
935 regulated genes. For example, in roots, 93 and 44 genes are respectively up- and down-regulated by
936 zinc deficiency (0 µM zinc) compared to the control condition (1.5 µM zinc) condition (root red square).
937 In shoots, these numbers are respectively 26 and 5 (shoot red square). (d) Ratios of common DEG to
938 the total number of unique DEG for five selected comparisons (deficiency vs. control, and four
939 consecutive comparisons upon zinc resupply) within each tissue are illustrated in green/brown cells.
940 These ratios are also expressed as percentage in each cell. The green upper half of the figure shows
941 shoot data, and the brown lower half shows root data. Color density illustrates the extent of DEG
942 overlap between two comparisons (a darker color corresponding to a larger overlap). The gray diagonal
943 cells present ratios of common DEG to the total number of unique DEG in each comparison between
944 root and shoot tissues.

945 **Figure 7.** Gene Ontology enrichment analysis of the steady-state response to zinc deficiency and excess
946 and the dynamic response to zinc deficiency and resupply in Brachypodium. The heatmaps present
947 statistically enriched (adj. $p < 0.05$) Biological Processes (BPs) among both up- and down-regulated
948 genes in 9 selected contrasts in roots (a) and in shoots (b). Each row shows a contrast. In the heatmap,
949 the color density indicates the statistical significance of the BP enrichment (-logarithm of adj. p-value),
950 while blue (down) and red (up) colors show the direction of regulation of genes involved in that BP
951 (each BP was specifically only up- or down- regulated with no genes behaving in the opposite direction
952 from that indicated).

953 **Figure 8.** Clustering of gene expression upon zinc deficiency and resupply in Brachypodium. Two
954 clusters containing differentially expressed *ZIP* genes in roots (a) and shoots (b) are shown. Pearson
955 correlation was used as distance metric in *k*-means clustering. The number of differentially expressed
956 genes included in each cluster is noted in each panel. Full clustering data of root and shoot DEGs are
957 shown in Fig. S6 and Fig. S7, respectively. Lines are there to indicate the expression profile of the genes
958 across the three biological replicates, and they should not be considered as time progression. The red
959 lines show the mean expression of all genes in the cluster.

960 **Figure 9.** Relative expression of metal homeostasis genes upon zinc deficiency and resupply in
961 Brachypodium. RNA sequencing (RNA-Seq, bottom plot) and quantitative RT-PCR (qPCR, top plot)
962 transcript levels are compared in roots and shoots for the Bradi1g17090 (NAS family), *BdHMA1*,
963 *BdIRT1*, *BdZIP13*, *BdZIP7* and *BdZIP4* genes. Bars show mean values (+/- standard deviation). qPCR

964 expression levels are relative to *UBC18* and *EF1α*, and scaled to average. RNA-Seq and qPCR data that
965 are from two fully independent experiments, each consisting of three biological replicates (2-4 plants
966 each). Letters indicate statistical differences (*p*-value < 0.05) according to one-way ANOVA.

967 **Figure 10.** ^{67}Zn labelling of Brachypodium plants upon zinc deficiency and resupply. Plants grown
968 hydroponically under zinc deficiency (0 µM Zn) for 3 weeks were resupplied with 1 µM ^{67}Zn and
969 samples were harvested after short time points (10 minutes to 8 hours). (a) Root, and (b) shoot ^{67}Zn
970 concentrations as determined by ICP-MS. (c) Shoot to root ^{67}Zn concentration ratio (Log) throughout
971 the time series upon ^{67}Zn resupply. Bars show mean values (+/- standard deviation) of three biological
972 replicates (4 plants each). Letters indicate statistical differences (*p*-value < 0.05) according to one-way
973 ANOVA.

974 **Figure 11.** Working model of root-to-shoot signaling upon zinc deficiency and resupply in
975 Brachypodium. (a) Zinc deficiency (0 Zn). Depletion of zinc in root and shoot causes strong upregulation
976 of *ZIP* genes in both tissues. (b) 10 minutes after zinc resupply (10 min). After a depletion period, zinc
977 resupply is sensed as stress (Zn shock) in roots which triggers rapid down-regulation of *ZIP* gene
978 expression in roots and initiates root-to-shoot signaling. In shoots, *ZIP* genes are also immediately
979 downregulated although zinc is not transported to shoot yet. (c) 30 minutes after zinc resupply (30
980 min). Zinc continues to accumulate in root cells, but remains at low concentration. *ZIP* genes are
981 upregulated again to sustain zinc uptake. This status is signaled to the shoot to induce a similar
982 response. (d) Five to eight hours after zinc resupply (5 h-8 h). Zinc concentration keeps increasing which
983 results in the downregulation of *ZIP* genes. At the same time, zinc is translocated to shoot (probably
984 by an HMA homolog; Bradi1g34140) and accumulation of zinc in shoot cells downregulates *ZIP* genes
985 in shoot as well though local signaling. Double-plus (++) shows very high quantity, plus (+) shows
986 moderate quantity, minus (-) shows low quantity and double-minus (--) shows very low quantity.

987

988

989

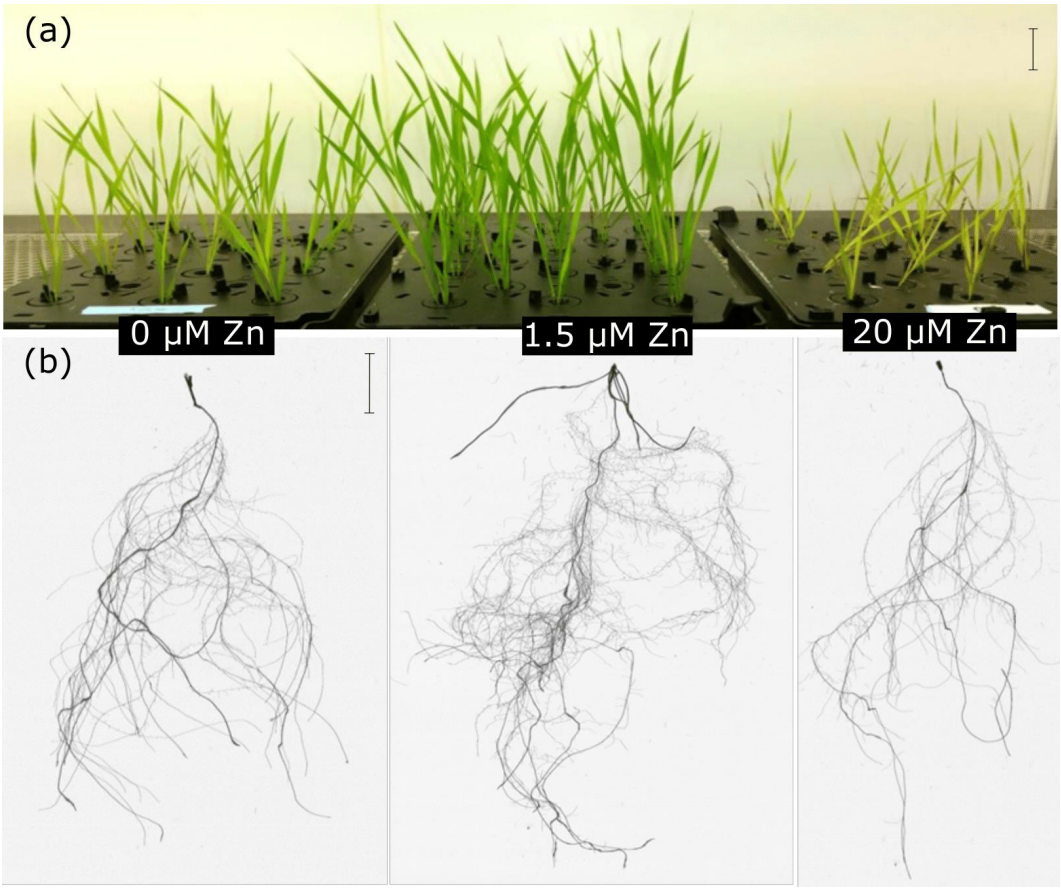

Figure 1. Brachypodium plants grown hydroponically in different zinc regimes for 3 weeks. (a) Shoot and (b) representative root images of plants exposed to zinc deficiency (0 µM Zn, left), control (1.5 µM Zn, center) or excess (20 µM Zn, right) conditions. Pictures are representative of multiple independent experiments. Scale bars are 2 cm.

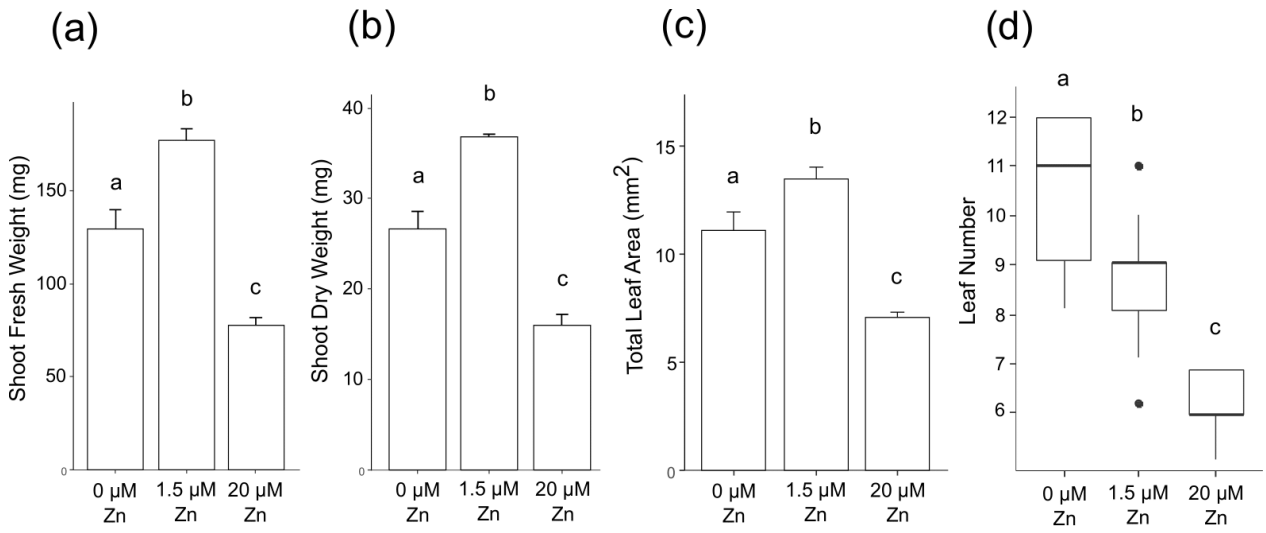

Figure 2. Shoot phenotype of Brachypodium plants upon zinc deficiency and excess. Plants grown hydroponically were exposed for 3 weeks to zinc deficiency (0 µM Zn), control (1.5 µM Zn) or excess (20 µM Zn) conditions. (a) Shoot fresh and (b) dry weight. (c) Total leaf area. (a-c) Bars show mean values (+/- standard deviation) of 9-12 individual plants for each treatment. (d) Leaf number per plant. Box and whisker plot showing the median (hardline), interquartile (box), 1.5 interquartile (whiskers) and outliers (dots) of values from 12 individual plants for each treatment. Letters indicate statistical differences (p-value < 0.05) according to Student's T-test.

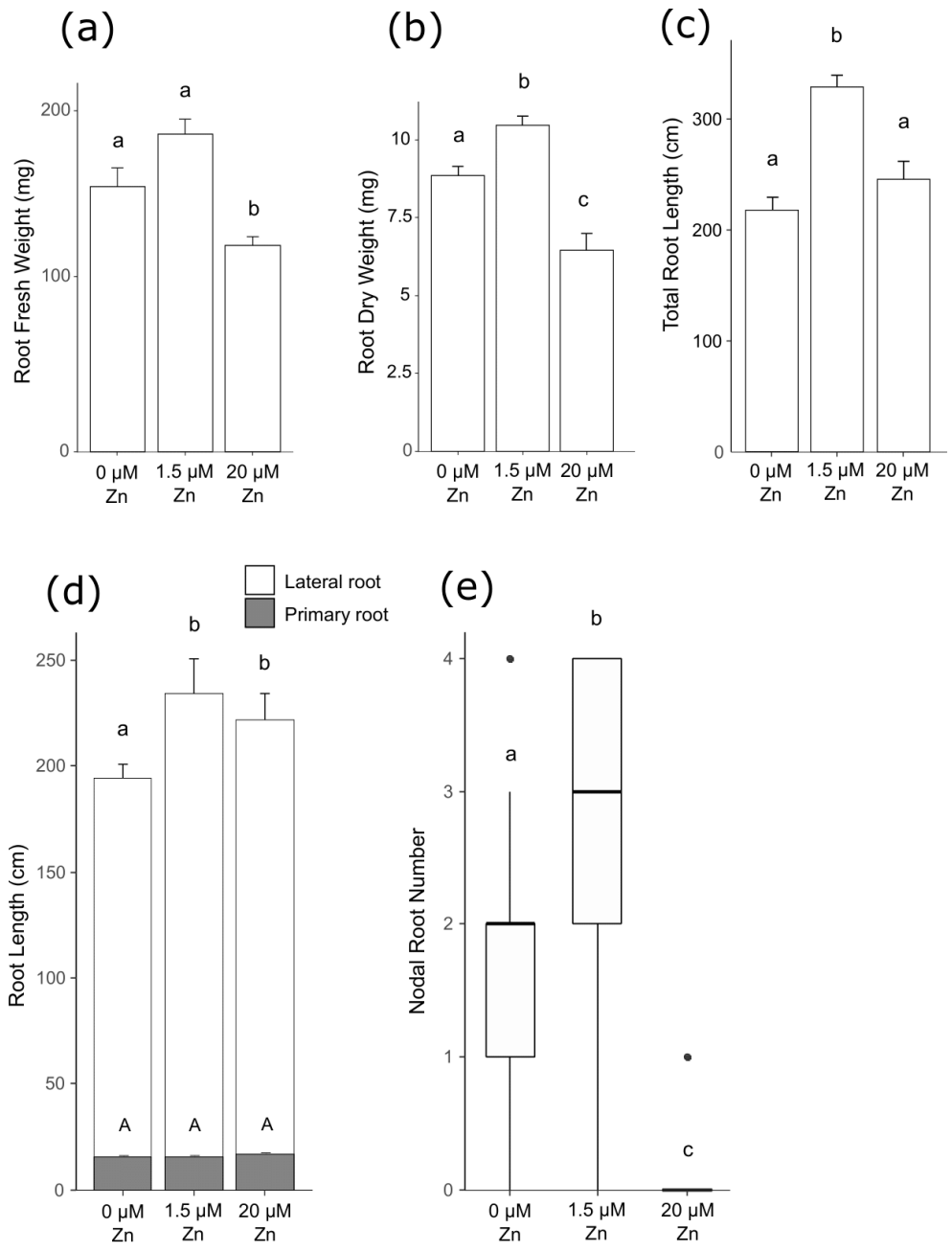

Figure 3. Root phenotypic measures of Brachypodium plants under three weeks of zinc treatments. Plants grown hydroponically were exposed for 3 weeks to zinc deficiency (0 µM Zn), control (1.5 µM Zn) or excess (20 µM Zn) conditions. (a) Root fresh weight, (b) root dry weight, (c) total root length and (d) primary and lateral root length. (a-d) Bars show mean values (+/- standard deviation) of 9-12 individual plants for each treatment. (e) Nodal root number per plant. Box and whisker plot showing the median (hardline), interquartile (box), 1.5 interquartile (whiskers) and outliers (dots) of values from 9 individual plants for each treatment. Letters indicate statistical differences (p-value < 0.05) according to Student's T-test.

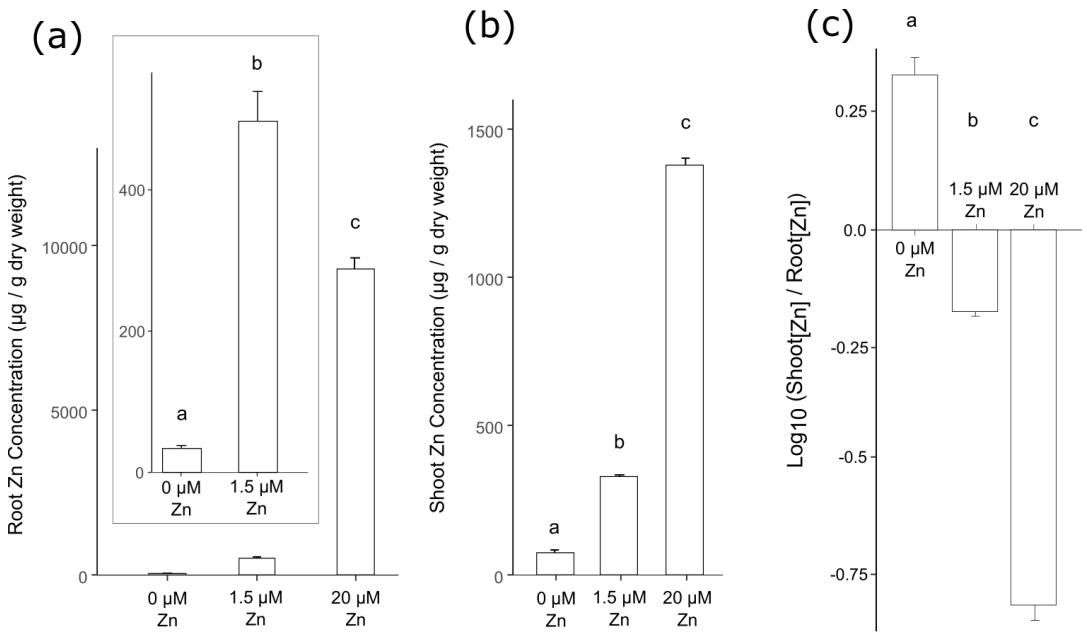

Figure 4. Zinc accumulation in roots and shoots of Brachypodium upon zinc deficiency and excess. Plants grown hydroponically were exposed for 3 weeks to zinc deficiency (0 µM Zn), control (1.5 µM Zn) or excess (20 µM Zn) conditions. (a) Root and (b) shoot zinc concentrations. (c) Shoot to root zinc concentration ratio (Log). Bars show mean values (+/- standard deviation) of three biological replicates (3-4 plants each). Letters indicate statistical differences (p-value < 0.05) according to Student's T-test.

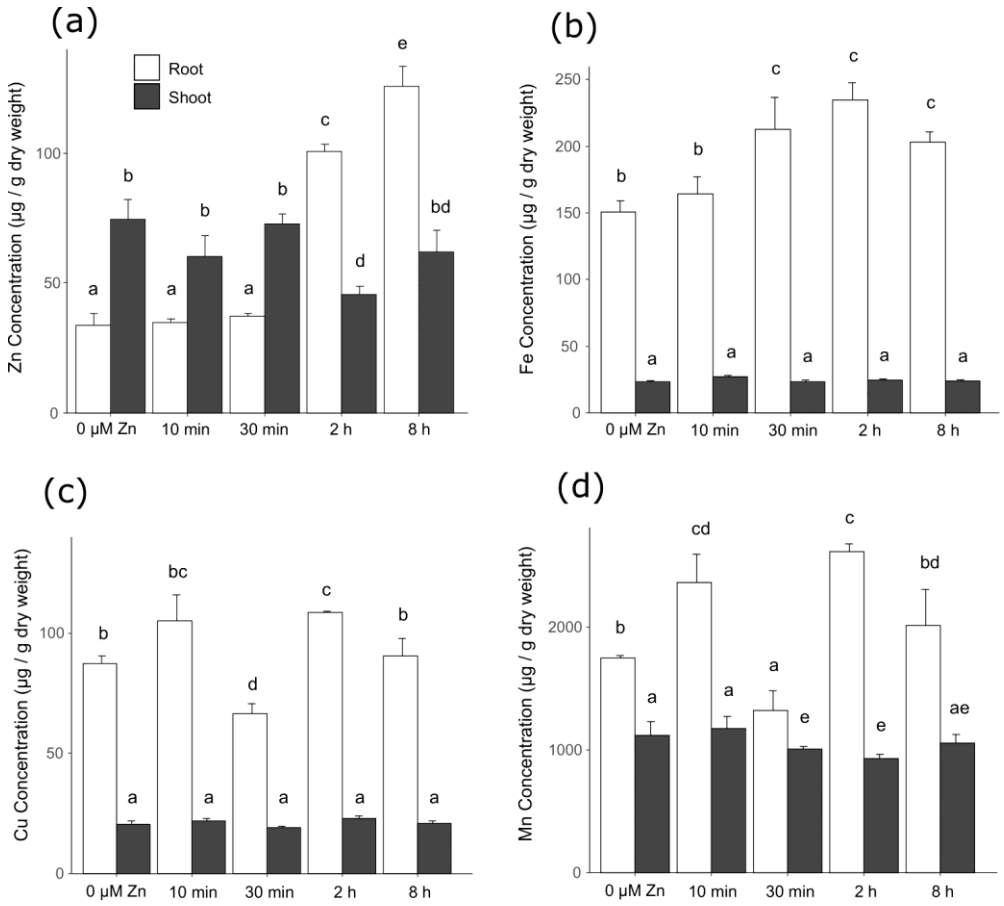

Figure 5. Ionome profiling of roots and shoots of Brachypodium upon zinc deficiency and re-supply. Plants grown hydroponically under zinc deficiency (0 µM Zn) for 3 weeks were resupplied with 1 µM Zn and samples were harvested after short time points (10 minutes to 8 hours). Root and shoot (a) zinc (Zn), (b) iron (Fe), (c) copper (Cu), and (d) manganese (Mn) concentrations. Bars show mean values (+/- standard deviation) of three biological replicates (3-4 plants each). Letters indicate statistical differences (*p*-value < 0.05) according to one-way ANOVA.

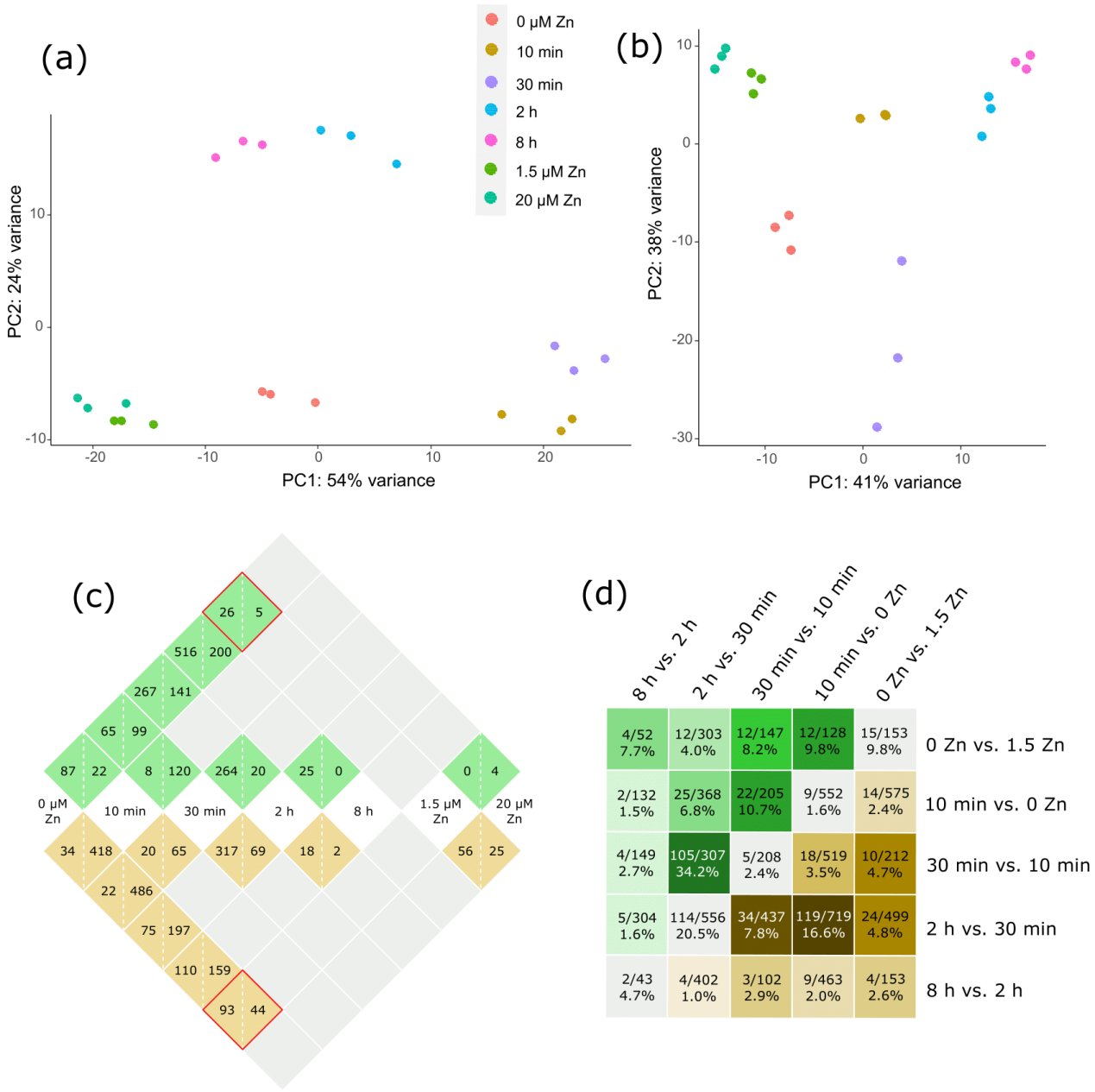

Figure 6. RNA sequencing analysis of the steady-state response to zinc deficiency and excess and the dynamic response to zinc deficiency and resupply in Brachypodium. Data are from three biological replicates (3-4 plants each) for each treatment. Principal Component Analysis (PCA) of (a) root and (b) shoot expression data. PCA of root and shoot data together is presented in Fig. S4. (c) Number of Differentially Expressed Genes (DEG) in 9 selected contrasts in roots (brown cells) and in shoots (green cells). Growth conditions are annotated in central white cells and DEGs identified in a contrast between 2 conditions are annotated in the intersecting cell, with numbers of up- (left) and down- (right) regulated genes. For example, in roots, 93 and 44 genes are respectively up- and down-regulated by zinc deficiency (0 µM zinc) compared to the control condition (1.5 µM zinc) condition (root red square). In shoots, these numbers are respectively 26 and 5 (shoot red square). (d) Ratios of common DEG to

the total number of unique DEG for five selected comparisons (deficiency vs. control, and four consecutive comparisons upon zinc resupply) within each tissue are illustrated in green/brown cells. These ratios are also expressed as percentage in each cell. The green upper half of the figure shows shoot data, and the brown lower half shows root data. Color density illustrates the extent of DEG overlap between two comparisons (a darker color corresponding to a larger overlap). The gray diagonal cells present ratios of common DEG to the total number of unique DEG in each comparison between root and shoot tissues.

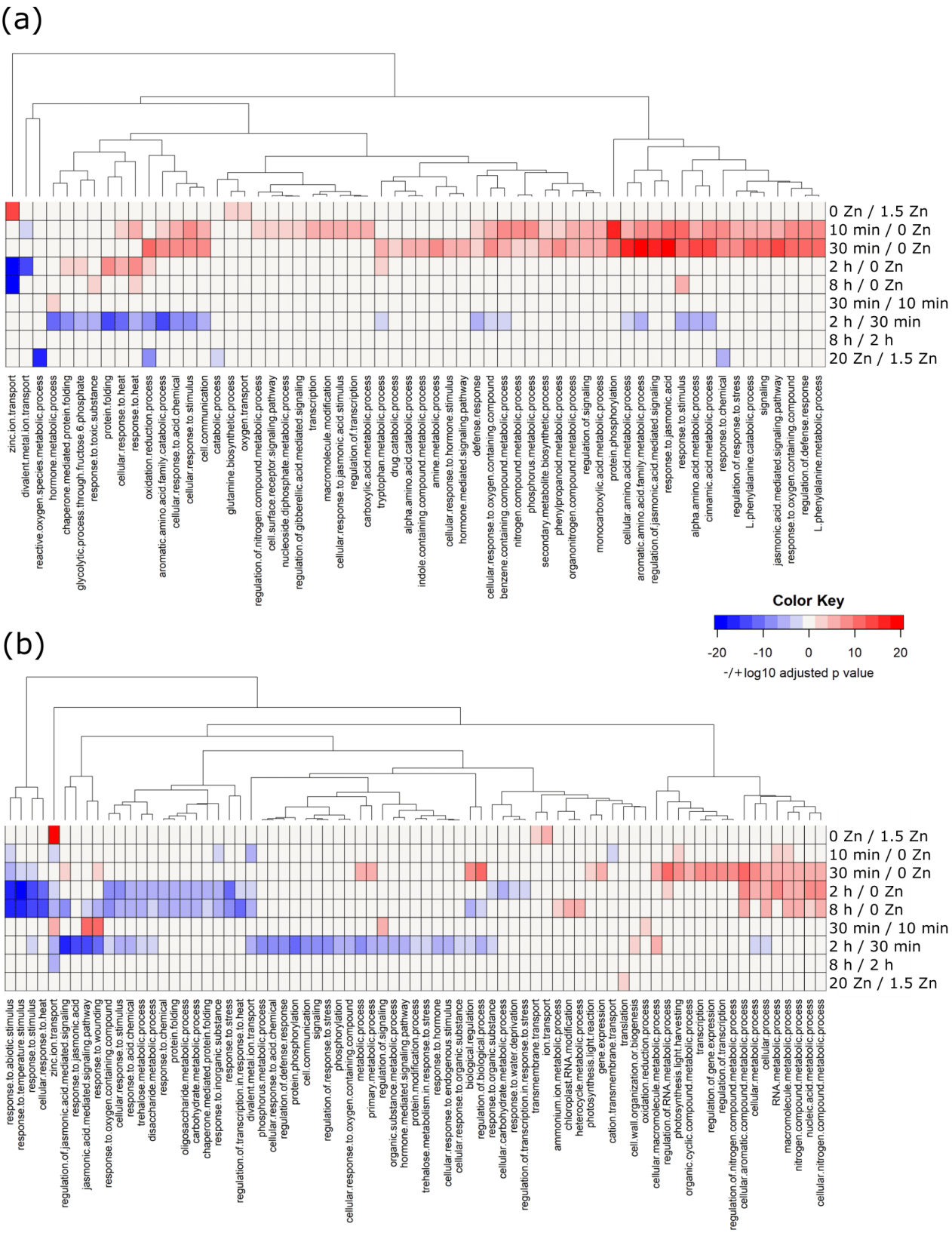

Figure 7. Gene Ontology enrichment analysis of the steady-state response to zinc deficiency and excess and the dynamic response to zinc deficiency and resupply in Brachypodium. The heatmaps present statistically enriched (adj. $p < 0.05$) Biological Processes (BPs) among both up- and down-regulated genes in 9 selected contrasts in roots (a) and in shoots (b). Each row shows a contrast. In the heatmap,

the color density indicates the statistical significance of the BP enrichment (-logarithm of adj. p-value), while blue (down) and red (up) colors show the direction of regulation of genes involved in that BP (each BP was specifically only up- or down- regulated with no genes behaving in the opposite direction from that indicated).

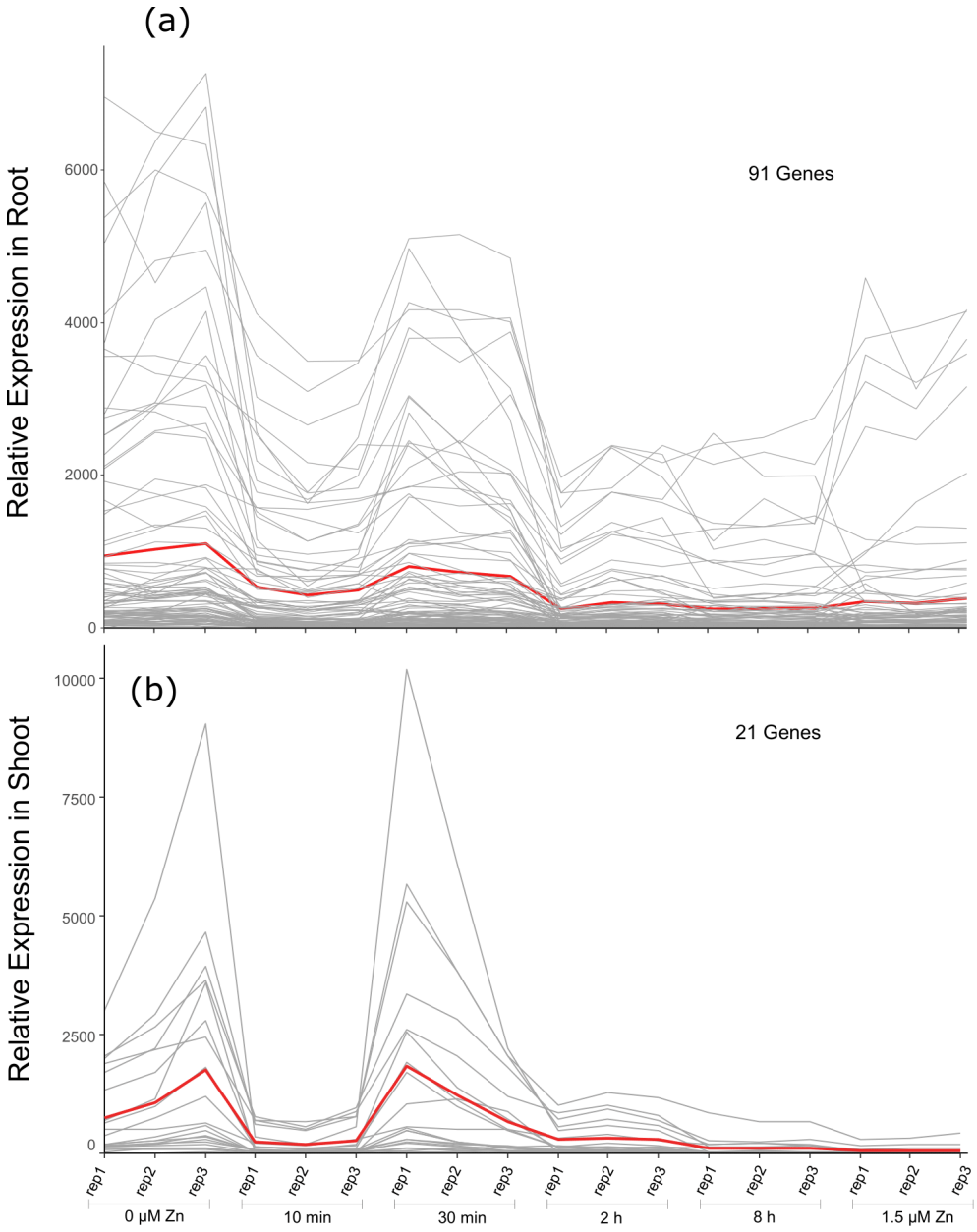

Figure 8. Clustering of gene expression upon zinc deficiency and resupply in Brachypodium. Two clusters containing differentially expressed *ZIP* genes in roots (a) and shoots (b) are shown. Pearson correlation was used as distance metric in *k*-means clustering. The number of differentially expressed genes included in each cluster is noted in each panel. Full clustering data of root and shoot DEGs are shown in Fig. S6 and Fig. S7, respectively. Lines are there to indicate the expression profile of the genes across the three biological replicates, and they should not be considered as time progression. The red lines show the mean expression of all genes in the cluster.

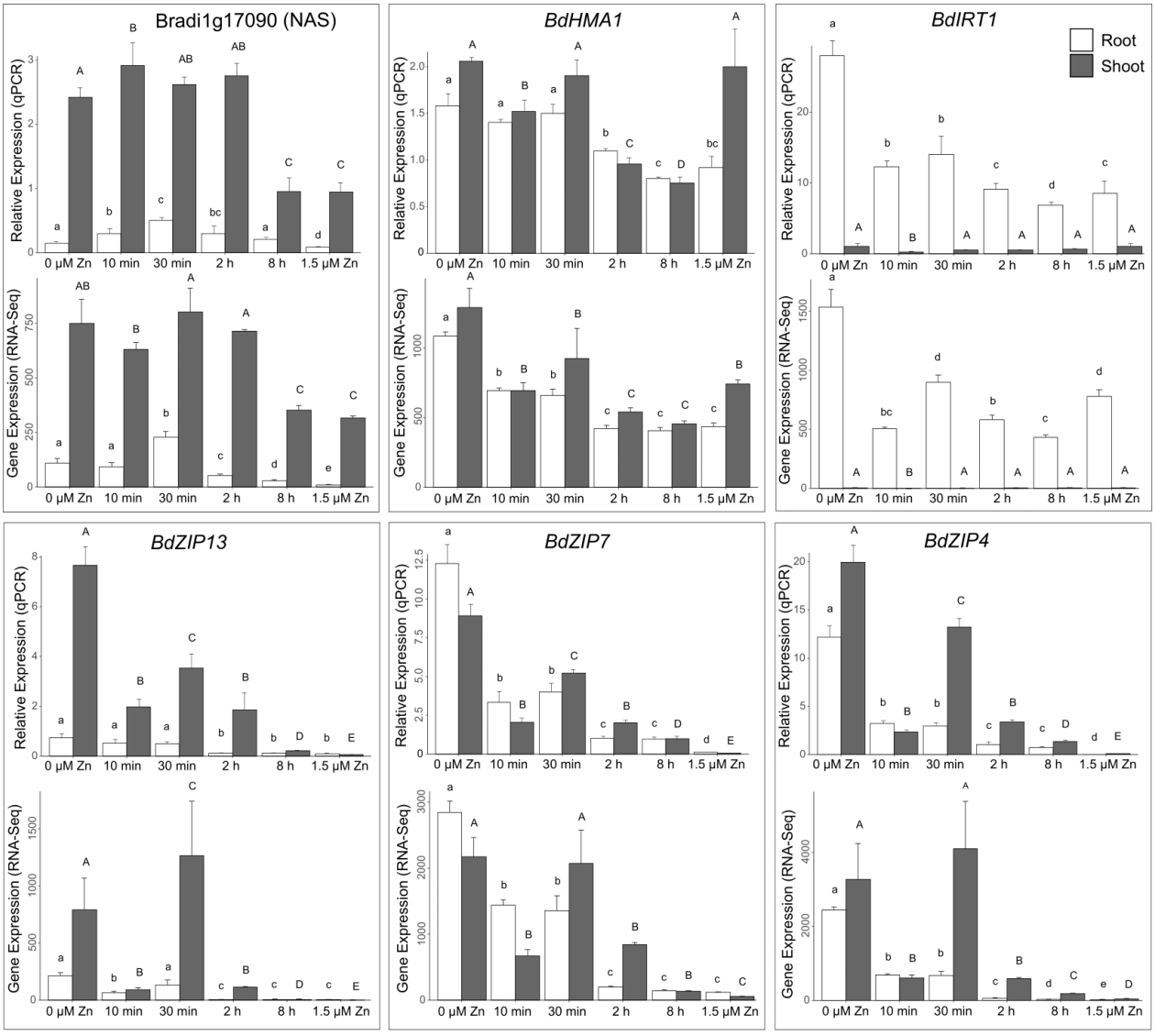

Figure 9. Relative expression of metal homeostasis genes upon zinc deficiency and resupply in Brachypodium. RNA sequencing (RNA-Seq, bottom plot) and quantitative RT-PCR (qPCR, top plot) transcript levels are compared in roots and shoots for the Bradi1g17090 (NAS family), *BdHMA1*, *BdIRT1*, *BdZIP13*, *BdZIP7* and *BdZIP4* genes. Bars show mean values (+/- standard deviation). qPCR expression levels are relative to *UBC18* and *EF1α*, and scaled to average. RNA-Seq and qPCR data that are from two fully independent experiments, each consisting of three biological replicates (2-4 plants each). Letters indicate statistical differences (p-value < 0.05) according to one-way ANOVA.

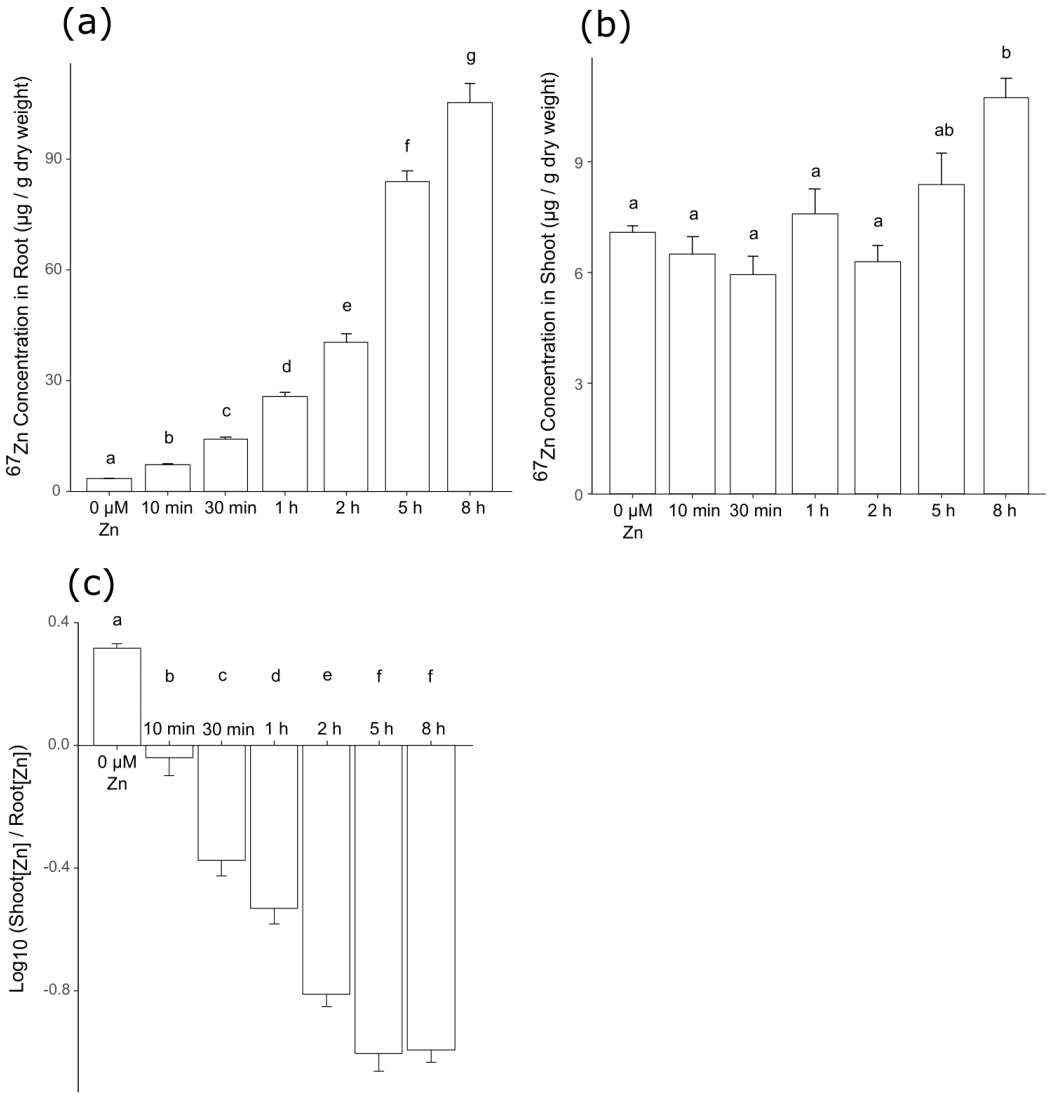

Figure 10. ^{67}Zn labelling of Brachypodium plants upon zinc deficiency and resupply. Plants grown hydroponically under zinc deficiency (0 µM Zn) for 3 weeks were resupplied with 1 µM ^{67}Zn and samples were harvested after short time points (10 minutes to 8 hours). (a) Root, and (b) shoot ^{67}Zn concentrations as determined by ICP-MS. (c) Shoot to root ^{67}Zn concentration ratio (Log) throughout the time series upon ^{67}Zn resupply. Bars show mean values (+/- standard deviation) of three biological replicates (4 plants each). Letters indicate statistical differences (p-value < 0.05) according to one-way ANOVA.

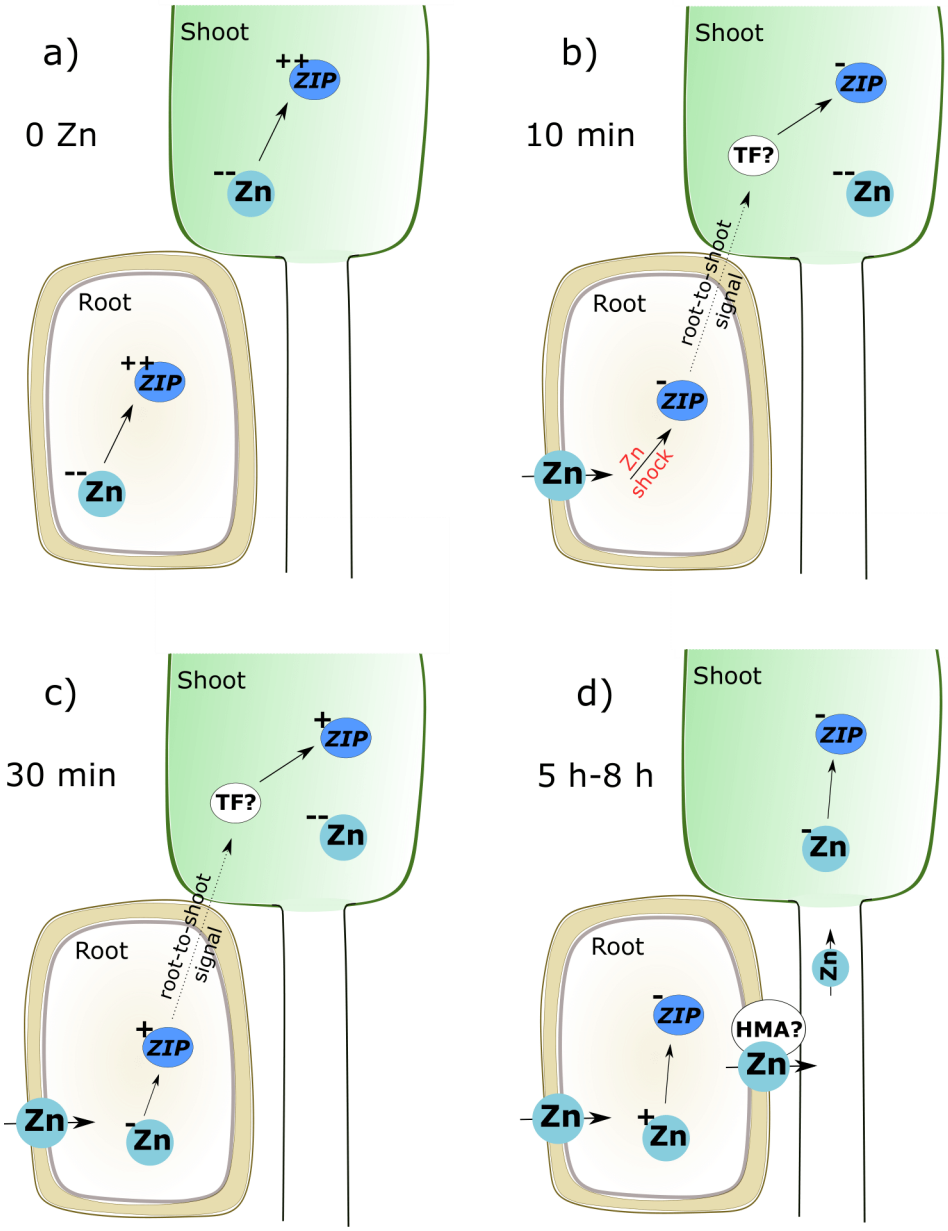

Figure 11. Working model of root-to-shoot signaling upon zinc deficiency and resupply in Brachypodium. (a) Zinc deficiency (0 Zn). Depletion of zinc in root and shoot causes strong upregulation of *ZIP* genes in both tissues. (b) 10 minutes after zinc resupply (10 min). After a depletion period, zinc resupply is sensed as stress (Zn shock) in roots which triggers rapid down-regulation of *ZIP* gene expression in roots and initiates root-to-shoot signaling. In shoots, *ZIP* genes are also immediately downregulated although zinc is not transported to shoot yet. (c) 30 minutes after zinc resupply (30 min). Zinc continues to accumulate in root cells, but remains at low concentration. *ZIP* genes are upregulated again to sustain zinc uptake. This status is signaled to the shoot to induce a similar response. (d) Five to eight hours after zinc resupply (5 h-8 h). Zinc concentration keeps increasing which results in the downregulation of *ZIP* genes. At the same time, zinc is translocated to shoot (probably by an HMA homolog; Bradi1g34140) and accumulation of zinc in shoot cells downregulates *ZIP* genes

in shoot as well though local signaling. Double-plus (++) shows very high quantity, plus (+) shows moderate quantity, minus (-) shows low quantity and double-minus (--) shows very low quantity.